3

Methods for Assessing Autophagy and Autophagic Cell Death

Ezgi Tasdemir, Lorenzo Galluzzi, M. Chiara Maiuri, Alfredo Criollo, Ilio Vitale, Emilie Hangen, Nazanine Modjtahedi, and Guido Kroemer

Summary

Autophagic (or type 2) cell death is characterized by the massive accumulation of autophagic vacuoles (autophagosomes) in the cytoplasm of cells that lack signs of apoptosis (type 1 cell death). Here we detail and critically assess a series of methods to promote and inhibit autophagy via pharmacological and genetic manipulations. We also review the techniques currently available to detect autophagy, including transmission electron microscopy, half-life assessments of long-lived proteins, detection of LC3 maturation/aggregation, fluorescence microscopy, and colocalization of mitochondrion- or endoplasmic reticulum–specific markers with lysosomal proteins. Massive autophagic vacuolization may cause cellular stress and represent a frustrated attempt of adaptation. In this case, cell death occurs *with* (or in spite of) autophagy. When cell death occurs *through* autophagy, on the contrary, the inhibition of the autophagic process should prevent cellular demise. Accordingly, we describe a strategy for discriminating cell death *with* autophagy from cell death *through* autophagy.

Key Words: Apoptosis; autophagosomes; fluorescence microscopy; endoplasmic reticulum; LC3-GFP; lysosomes; mitochondria; starvation.

1. Introduction

Autophagy is an evolutionarily conserved, homeostatic process that allows for the bulk degradation of long-lived proteins and organelles ***(1)***. In eukaryotic cells, the autophagic pathway is initiated when organelles and/or portions of the cytosol destined to degradation are enclosed within double-membraned vacuoles, namely autophagosomes (also known as AV, i.e., autophagic vacuoles). To promote the

From: *Methods in Molecular Biology, vol. 445: Autophagosome and Phagosome*
Edited by: V. Deretic © Humana Press, Totowa, NJ

degradation of their luminal content, autophagosomes fuse with lysosomes, thus forming the so-called autophagolysosomes ***(2)***. It is important to note that the mere presence of AV in cells is not a proof of elevated autophagy, because a reduced turnover of AV (e.g., due to a decreased fusion of AV with lysosomes) suffices to increase their number severalfold ***(3)***. Accordingly, ultrastructural studies have to be accompanied by evidence for increased protein and/or organelle turnover to ascertain increased autophagic activity.

The execution and regulation of the autophagic program rely on several autophagy-specific genes (*atg*), which are characterized by a high degree of conservation among species as distant as humans and yeast ***(4)***. Some Atg proteins are directly implicated in the formation of the autophagosome. For instance, the ubiquitination of Atg5 and Atg12 by the E1-like enzymes Atg7 and Atg10 is required to form AV ***(5)***. Microtubule-associated protein light chain 3 (LC3) is the mammalian equivalent of yeast Atg8 and exists in two forms, LC3-I and -II. LC3-I is an 18-kDa polypeptide normally found in the cytosol, whereas the product of its proteolytic maturation (LC3-II, 16 kDa) resides in the autophagosomal membranes ***(6)***. Beclin-1 is the mammalian orthologue of yeast Atg6 and localizes to the trans-Golgi network, where it participates in autophagosome formation by interacting with the class III phosphatidylinositol 3-kinase (PI3K) human vacuolar protein sorting factor protein 34 (hVps34) ***(7)***. Importantly, the pro-autophagic interaction between hVps34 and Beclin-1 can be inhibited by the binding of the latter to the anti-apoptotic proteins Bcl-2 or Bcl-Xʟ ***(8)***.

To ensure the turnover of old and damaged organelles, autophagy occurs constitutively at low, basal levels. However, it is also a tightly regulated adaptive mechanism that enhances cell survival under various environmental and cellular stresses, including nutrient deprivation, oxidative stress, accumulation of misfolded proteins, bacterial and viral infection, toxic stimuli, and irradiation ***(9,10)***. One of the most efficient triggers of autophagy is starvation. In response to culture in nutrient-free media, cells degrade nonessential components to meet the cell's energetic demand as well as to provide metabolites for vital biosynthetic reactions. In this scenario, the suppression of autophagy by chemical inhibitors or by the downregulation of essential genes (e.g., Atg5, Atg6/Beclin-1, Atg10, or Atg12) can sensitize cells to starvation-induced death ***(3)***. Autophagy inhibition sensitizes cells also to the depletion of obligatory growth (or survival) factors, which result in decreased nutrient import through the plasma membrane. This cell death occurs without massive autophagic vacuolization and is usually accompanied by the hallmarks of apoptosis, including mitochondrial membrane permeabilization (MMP) and activation of caspases ***(3)***. In some instances, the inhibition of autophagy tends to shift the cell death subroutine to more necrotic phenotypes ***(11)***.

A very different picture emerges when the late stages of AV maturation (e.g., fusion between AV and lysosomes) are inhibited. This may be accomplished by the administration of lysosomotropic bases (hydroxychloroquine or chloroquine) ***(3)***, by inhibiting the vacuolar proton pump responsible for the luminal acidification of lysosomes (with bafilomycin A1) ***(3)***, or by the knock-down of the gene encoding lysosome-associated membrane protein 2 (LAMP-2) ***(12)***. In such conditions, nutrient-starved cells massively accumulate AV in the cytoplasm, as determined by electron microscopy or by following the redistribution of the AV marker LC3 fused with a green fluorescent protein (GFP) moiety (LC3-GFP). In spite of AV accumulation, the autophagic protein turnover is inhibited ***(12,13)***. This example illustrates the importance of using a correct combination of methods to assess AV formation, AV turnover, and cell death.

In some cases, cells manifesting massive autophagic vacuolization can be rescued from cell death by the removal of lysosomal inhibitors and/or the readdition of nutrients, despite their sometimes disastrous morphological aspect evoking textbook images of autophagic cell death. This is especially true when the still nucleus exhibits a normal aspect and mitochondria remain energized ***(14)***. However, upon prolonged nutrient starvation and inhibition of the formation of autophagolysosomes, vacuolated cells manifest the hallmarks of apoptosis (e.g., MMP, release of toxic proteins from the mitochondrial intermembrane space, and caspase activation), indicating that the point of no return that separates cellular life and death has been trespassed ***(15)***.

Autophagy has been suggested to constitute an effector mechanism of cell death, meaning that self-eating would be the first step of self-killing. Some pharmacological studies based on the use of 3-methyladenine (3-MA, a low-affinity inhibitor of hVps34) tend to support this hypothesis. For instance, it has been proposed that autophagy is required for the death of sympathetic neurons cultured in the absence of the essential nerve cell growth factor (NGF) and in the presence of caspase inhibitors ***(16)***. Similarly, TRAIL-induced autophagy accounts for the formation of hollow acini-like structures in differentiating mammary epithelial cells ***(17)***. In this model, 3-MA can provoke luminal filling when caspase-3 is inhibited by overexpression of a Bcl-Xl transgene. However, the fact that 3-MA effectively inhibits hVps34 only at concentrations $\geq$10 m*M* sheds major doubts on its specificity. Reportedly, inhibition of Atg genes by small interfering RNAs (siRNAs) can prevent autophagic cell death, at least in some models. For instance, siRNA-mediated downregulation of Atg6/Beclin-1 or Atg7 has been shown to reduce type 2 cell death of human U937 cells dying in response to caspase-8 inhibition ***(18)***. siRNAs targeting Atg6/Beclin-1 and Atg5 are able to prevent the autophagic cell death of $Bax^{-/-}Bak^{-/-}$ mouse embryonic fibroblasts succumbing to the inhibition of topoisomerase 2 by

etoposide or to inhibition of tyrosine kinases by staurosporine ***(19)***. Finally, knock-down of Atg5 (or overexpression of a dominant negative variant of Atg5) can inhibit interferon-γ (IFN-γ)–induced autophagic vacuolization and subsequent cell death ***(20)***.

The definition of the features that may be employed to identify dead cells has been the subject of a long debate. Permeabilization of the plasma membrane, disintegration of the cell, and/or phagocytosis of the corpse have been recognized as the characters that delimit the irreversibility of the process ***(21,22)***. Several subroutines of cell death can be distinguished according to ultrastructural criteria. The best-studied modality of cell death, apoptosis (type 1 cell death), is characterized by morphological changes that include nuclear pyknosis (chromatin condensation) and karyorhexis (nuclear fragmentation). As the process advances, cells form small round bodies surrounded by membranes that contain intact cytoplasmic organelles and/or nuclear fragments. In vivo, these "apoptotic bodies" are usually engulfed by resident phagocytic cells. As mentioned above, massive autophagic vacuolization is observed in some instances of cell death, which has been named "autophagic cell death" (type 2 cell death) ***(22)***. It is an ongoing conundrum, however, in which case "autophagic cell death" is truly mediated *through* autophagy (meaning that its inhibition would prevent cell death) and in which case it simply occurs together *with* autophagy (meaning that inhibition of autophagy would affect only the morphology of the process, but not the fate of cells) ***(12,23)***. Necrosis (type 3 cell death) is a subroutine of cell death that does not manifest the hallmarks of apoptosis or massive autophagic vacuolization. The principal feature of necrosis is a gain in cell volume (oncosis) that finally culminates in the sudden rupture of the plasma membrane, accompanied by the unorganized dismantling of swollen organelles ***(11)***.

In spite of the large amount of published data, the methods that are currently available for the detection of autophagy are affected by numerous intrinsic pitfalls. The most reliable and conventional technique to visualize autophagic vacuolization is transmission electron microscopy. Biochemical methods and techniques designed to measure the aggregation of autophagosome markers allow for the monitoring of autophagy, yet are afflicted by relevant problems. Here, we will provide an overview of routine methods for the assessment of autophagy and autophagic cell death.

2. Materials

2.1. Common Materials

2.1.1. Disposables

1. 1.5-mL microcentrifuge tubes (Eppendorf, Hamburg, Germany).100 × 20 culture dishes (Corning Inc. Life Sciences, Acton, MA).

2. 12-mm Ø cover slips (Menzer-Gläser GmbH, Braunschweig, Germany)—sterilized by incubation for 15–30 min in 100% ethanol (Carlo Erba Reagents, Milan, Italy).
3. 15- and 50-mL conical centrifuge tubes (BD Falcon, San Jose, CA). 175-cm^2 flasks for cell culture (BD Falcon).
4. 5-mL, 12 × 75 mm FACS tubes (BD Falcon).
5. 6-, 12-, 24-well plates for cell culture (Corning Inc. Life Sciences).
6. 76 × 26 mm slides for fluorescence microscopy (Carl Roth GmbH, Karlsruhe, Germany).

2.1.2. Solutions

1. Growth medium for HeLa cells: Dulbecco's modified Eagle's medium (DMEM) containing 4.5 g/L glucose, 4 m*M* L-glutamine and 110 mg/L sodium pyruvate (Gibco-Invitrogen, Carlsbad, CA) supplemented with 100 m*M* HEPES buffer (Gibco-Invitrogen) and 10% fetal bovine serum (FBS, from PAA Laboratories GmbH, Pasching, Austria).
2. PBS (1X): 137 m*M* NaCl, 2.7 m*M* KCl, 4.3 m*M* Na_2HPO_4, 1.4 m*M* KH_2PO_4 in deionized water (dH_2O), adjust pH to 7.4 with 2 *N* NaOH.
3. Trypsin/ethylenediaminetetraacetic acid (EDTA): 0.25% trypsin, 0.38 g/L (1mM) EDTA•4Na in Hank's balanced salt solution (HBSS) (Gibco-Invitrogen).

2.2. Experimental Modulation of Autophagy

1. Autophagy inducers are listed in **Table 1**.
2. Autophagy inhibitors are listed in **Table 2**.
3. siRNAs used for the inhibition of the autophagic pathway in human cell lines are reported in **Table 3**.
4. Oligofectamine™ transfection reagent (Oligofectamine™, from Gibco-Invitrogen).
5. Opti-MEM®reduced serum medium (Opti-MEM®), with Glutamax™ and phenol red (Gibco-Invitrogen).

2.3. Measuring Autophagy

1. 3 MM® Whatmann filter paper.
2. 40% acrylamide:*N-N'*-methylenediacrylamide (29/1) solution (Bio-Rad, Hercules, CA).
3. 6-mm-thick, 10.5 × 11 cm foam sponges (GE Healthcare Life Sciences Sciences, Uppsala, Sweden).
4. Ammonium persulfate (APS), stock solution at 10% (w/v) in dH_2O (stored at 4°C) (*see also* **Note 37**).
5. Antibodies employed in immunoblotting techniques are listed in **Table 4**.
6. Blocking buffer: 0.1% Tween-20 (Sigma-Aldrich) and 5% (w/v) nonfat powdered milk (commonly found in food stores) in PBS. Storage at 4°C should not exceed one week, unless 0.02% sodium azide is added as preservative.

Table 1
Autophagy Inducers

Reagent	Company[a]	Activity	Stock solution storage	Final concentration
Brefeldin A	Sigma-Aldrich	ER stressing agent	10 m*M* in ethanol −20°C	20 μ*M*
Carbamazepine	Sigma-Aldrich	IMPase inhibitor	5 m*M* in ethanol −20°C	50 μ*M*
Earle's Balanced Salt Solution	Sigma-Aldrich	Starvation inducer (NF medium)	4°C	100%
L-690,330	Tocris Biosciences	IMPase inhibitor	10 m*M* in dH_2O −20°C	100 μ*M*
Lithium Chloride	Sigma-Aldrich	IMPase inhibitor	1 *M* in dH_2O4°C	10 m*M*
N-Acetyl-D-sphingosine (C2-ceramide)	Sigma-Aldrich	Class I PI3K pathway inhibitor	10 m*M* in DMSO −20°C	75–100 μ*M*
Rapamycin	Tocris Biosciences	mTOR inhibitor	1 m*M* in DMSO −20°C	1 μ*M*
Thapsigargin	Calbiochem	ER stressing agent	1 m*M* in DMSO −20°C	3 μ*M*
Tunicamycin	Sigma-Aldrich	ER stressing agent	1 m*M* in DMSO −20°C	2.5 μ*M*
Xestospongin B	Not available for purchase	IP_3R blocker	2 m*M* in ethanol −20°C	2 μ*M*
Xestospongin C	Calbiochem	IP_3R blocker	2 m*M* in ethanol −20°C	10 μ*M*

[a]Calbiochem, San Diego, CA; Sigma-Aldrich, St. Louis, MO; Tocris Biosciences, Ellisville, MO.

Table 2
Autophagy inhibitors

Reagent	Company[a]	Activity	Stock solution Storage	Final concentration
3-Methyladenine (3-MA)	Sigma-Aldrich	hVps34 inhibitor	Powder RT	10 m*M*
Bafilomycin A1	Sigma-Aldrich	H^+-ATPase inhibitor	0.2 m*M* in DMSO −20°C	0.1 μ*M*
Hydroxy-chloroquine	Sanofi-Aventis	Lysosomal lumen alkalizer	30 mg/mL in dH_2O −20°C	30 μg/mL

[a]Sanofi- Aventis, Bridgewater, NJ; Sigma-Aldrich, St. Louis, MO.

7. Bovine serum albumin (BSA, from Sigma-Aldrich), stock solution 10 mg/mL in dH_2O, stored at 4°C).
8. Chemiluminescent substrate: SuperSignal West Femto Maximum Sensitivity Substrate (Pierce Biotechnology, Rockford, IL).
9. Chemiluminescent substrate: SuperSignal West Pico Chemiluminescent Substrate (Pierce Biotechnology).
10. *DC* protein assay (Bio-Rad).
11. Dehybridizing buffer: 570 μL of 1 *N* acetic acid solution (Sigma-Aldrich) + 100 mL dH_2O.
12. Electrophoresis apparatus: Mini-PROTEAN 3 electrophoresis cell system (Bio-Rad), powered by a PowerPac HC power supply (Bio-Rad).
13. Epon® epoxy resin (Miller-Stephenson, Danbury, CT).
14. Film processor: Curix 60 table-top film processor (Agfa, Mortsel, Belgium).
15. Fixative solution: 4% paraformaldehyde (PFA, from Sigma-Aldrich) + 0.19% picric acid (Sigma-Aldrich) in PBS. For 10 mL: dissolve 0.4 g of PFA in 500 μL of dH_2O, add one drop of 2 *N* NaOH, heat to 65–70°C until solution clears, add 9.5 mL of PBS, let cool to room temperature (RT), add 38 μL of saturated picric acid (Sigma-Aldrich), and move the fixative solution to ice bath (*see also* **Notes 13–15**).
16. Fluorescence microscope: IRE2 microscope equipped with a DC300F camera (Leica Microsystems GmbH, Wetzlar, Germany).
17. Fluorescent dyes used for the detection of autophagy are listed in **Table 5**.
18. Fluoromount-G™ mounting medium (Southern Biotech, Birmingham, AL).
19. Grade I glutaraldehyde solution, 25% in dH_2O, specially purified for use as an electron microscopy fixative (Sigma-Aldrich).
20. Isopropyl alcohol (isopropanol, CAS No. 67-63-0, from Carlo Erba Reagents).
21. l-[U-^{14}C]-Valine, aqueous solution containing 2% ethanol, sterilized (GE Healthcare Life).

Table 3
siRNAs Used to Knock Down Genes Involved in utophagy in Human Cell Lines

Target gene	Symbol	Accession number	Sequence	Ref.
Autophagy related gene 5 homolog	*atg5*	BC002699	sense 5'-GCAGAACCAUACUAUUUGCdTdT-3' antisense 5'-GCAAAUAGUAUGGUUCUGCdTdT-3' sense 5'-GCAACUCUGGAUGGGAUUGdTdT-3' antisense 5'-CAAUCCCAUCCAGAGUUGCdTdT-3'	***(3)***
Autophagy related gene 10 homolog	*atg10*	NM_8031482	sense 5'-GGAGUUCAUGAGUGCUAUAdTdT-3' antisense 5'-GUAGCCAUCAGAACAGUCCdTdT-3' sense 5'-GGACUGUUCUGAUGGCUACdTdT-3' antisense 5'-GUAGCCAUCAGAACAGUCCdTdT-3'	***(3)***
Autophagy related gene 12 homolog	*atg12*	NM_004707	sense 5'-CAGAGGAACCUGCUGGCGAdTdT-3' antisense 5'-UCGCCAGCAGGUUCCUCUGdTdT-3' sense 5'-GAAGUUGGAACUCUCUAUGdTdT-3' antisense 5'-CAUAGAGAGUUCCAACUUCdTdT-3'	***(3)***
Beclin-1	*atg6*	AF077301	sense 5'-CUCAGGAGAGGAGCCAUUUdTdT-3' antisense 5'-AAAUGGCUCCUCUCCUGAGdTdT-3' sense 5'-GAUUGAAGACACAGGAGGCdTdT-3' antisense 5'-GCCUCCUGUGUCUUCAAUCdTdT-3'	***(3)***
Emerin	*emd*	NC_000023.9	sense 5'-CCGUGCUCCUGGGGCUGGGdTdT-3' antisense 5'-CCCAGCCCCAGGAGCACGGdTdT-3'	***(81)***

Human vacuolar protein sorting factor protein 34	*hVps34*	NM_002647	sense 5'-GGCUGAAACUACCAGUAAAdTdT-3' antisense 5'-UUUACUGGUAGUUUCAGCCdTdT-3' sense 5'-GGAGGCAAAUAUCCAGUUAdTdT-3' antisense 5'-UAACUGGAUAUUUGCCUCCdTdT-3'	***(82)***
Lysosome-associated membrane protein 1	*lamp-1*	NM_005561	sense 5'-CGAGAAAUGCAACACGUUAdTdT-3' antisense 5'-UAACGUGUUGCAUUUCUCGdTdT-3' sense 5'-GGAAUCCAGUUGAAUACAAdTdT-3' antisense 5'-UUGUAUUCAACUGGAUUCCdTdT-3'	***(12)***
Lysosome-associated membrane protein 2	*lamp-2*	NM_002294	sense 5'-GCUGUGCGGUCUUAUGCAUdTdT-3' antisense 5'-AUGCAUAAGACCGCACAGCdTdT-3' sense 5'-GCGGUCUUAUGCAUUGGAAdTdT-3' antisense 5'-UUCCAAUGCAUAAGACCGCdTdT-3'	***(12)***

Notes: siRNAs are provided either as 100 m*M* stock solutions (to be stored as such at −20°C), or in dehydrated form. In the latter case, stock solutions should be prepared by adding an appropriate volume of dH_2O or of the specific basic buffer (usually delivered with the siRNA) to obtain the final siRNA concentration of 20–100 m*M*, and by incubating the tube first at 90°C for 1 min then at 37°C for 1 h. These steps are required to resolve secondary structures that may have formed during lyophilization and that may interfere with the siRNA silencing efficacy.

Table 4
Antibodies for Immunoblotting

Primary antibody	Specificity	Source organism	Company[a]	Ref.
Anti-GAPDH (6C5)	Monoclonal IgG_1	Mouse	Chemicon International	mAB374
Anti-LC3	Polyclonal IgG	Rabbit	Santa Cruz Biotechnology	sc-28266
Secondary antibody	**Label**	**Source organism**	**Company[a]**	**Ref.**
Anti-mouse	Horseradish peroxidase	Goat	Southern Biotech	1010-05
Anti-rabbit	Horseradish peroxidase	Goat	Southern Biotech	4010-05

[a]Chemicon International, Temecula, CA; Santa Cruz Biotechnology, Santa Cruz, CA; Southern Biotech, Birmingham, AL.

22. Lead citrate: dissolve 0.1 g of lead(II) citrate tribasic trihydrate (Sigma-Aldrich) in 100 mL dH_2O; add dropwise 10 *N* NaOH (Sigma-Aldrich) until solution becomes clear; store at RT.
23. Lipofectamine™ 2000 transfection reagent (Lipofectamine™, from Gibco-Invitrogen).
24. Loading buffer (5X): 313 m*M* Tris-HCl (pH 6.8), 10 m*M* EDTA, 500 m*M* DL-dithiothreitol (DTT), 10% (w/v) sodium dodecylsulfate (SDS), 50% (v/v) glycerol, 0.05% (w/v) bromophenol blue in dH_2O (or commercially available from Fermentas, Ontario, Canada).
25. L-Valine (Sigma-Aldrich), stock solution in dH_2O, at the concentration of 100 m*M* (stored at 4°C).
26. Lysis buffer: CelLytic™ M (Sigma-Aldrich).
27. Migration buffer (1X): 100 mL 10X Tris/Glycine/SDS buffer (Bio-Rad) + 900 mL dH_2O.
28. Mini-PROTEAN 3 combs (5-, 9- 10- or 15- wells, from Bio-Rad) (*see also* **Note 46**).
29. *N,N,N',N'*-Tetra-methyl-ethylenediamine (TEMED, from Bio-Rad).
30. Nitrocellulose membrane roll (Bio-Rad).
31. Osmium tetroxide solution for electron microscopy, 2% in dH_2O.
32. Photographic films: 18 × 24 Amersham Hyperfilm™ ECL™ (GE Healthcare Life Sciences).

Table 5
Fluorescent Probes, Labels, and Proteins for the Detection of Autophagy and Autophagic Cell Death

Fluorescent probes	Absorption peak	Emission peak	Color	Application	Company[a]	Stock solution Storage[b]	Final concentration
CellTracker™ Green (CMFDA)	492 nm	517 nm	Green	IF	Molecular Probes	10 m*M* in DMSO –20°C	1 μ*M*
DiOC3 ***(6)***	484 nm	501 nm	Green	FACS (FL1 channel)	Molecular Probes	40 μ*M* in ethanol –20°C	40 n*M*
EthBr (bound to DNA)	300 nm	603 nm	Red	FACS (FL3 channel)	Not applicable[c]	Not applicable[c]	Not applicable[c]
HE	[4]518 nm	420 nm[d]	Blue[d]	not applicable[d]	Molecular Probes	5 m*M* in DMSO –20°C	25 μ*M*
Hoechst 33342 (bound to DNA)	352 nm	461 nm	Blue	IF	Molecular Probes	10 mg/mL in dH_2O 4°C	2 μ*M*
LysoTracker® Red	577 nm	590 nm	Red	IF	Molecular Probes	1 m*M* in DMSO –20°C	50–75 n*M*
MDC (in AV)	335 nm	[5]498 nm[e]	Green	IF	Sigma-Aldrich	5 m*M* in 1:1 DMSO/ethanol Freshly made	50 μ*M*
MitoTracker® Red (CMXRos)	579 nm	599 nm	Red	IF	Molecular Probes	1 m*M* in DMSO –20°C	150 n*M*
NAO	500 nm	520 nm	Green/Red	FACS (FL1/2 channel)	Molecular Probes	500 μ*M* in ethanol –20°C	100 n*M*
PI	535 nm	617 nm	Red	FACS (FL3 channel)	Sigma-Aldrich	1 mg/mL in dH_2O	1 μg/mL

TMRM	543 nm	573 nm	Red	FACS (FL2 channel)	Molecular Probes	15 m*M* in ethanol –20°C	150 n*M*

Fluorescent labels	Absorption peak	Emission peak	Color	Application	Company[a]	Coupling
Alexa Fluor®488	495 nm	519 nm	Green	IF	Molecular Probes	Secondary antibodies (goat anti-mouse)
Alexa Fluor®568	578 nm	603 nm	Red	IF	Molecular Probes	Secondary antibodies (goat anti-mouse and anti-rabbit)
FITC	494 nm	519 nm	Green	FACS (FL1 channel)	Miltenyi Biotec	Annexin V

Fluorescent proteins	Absorption peak	Emission peak	Color	Application	Company[a]	Coupling
DsRed2	558 nm	583 nm	Red	IF	Clontech Laboratories	mito
GFP	488 nm	507 nm	Green	IF	Clontech Laboratories	LC3

[a]Clontech Laboratories, Palo Alto, CA; Miltenyi Biotec, Bergisch Gladbach, Germany; Molecular Probes-Invitrogen, Carlsbad, CA; Sigma-Aldrich, St. Louis, MO.
[b]To avoid photobleaching, all stock solutions should be stored under protection from light.
[c]EthBr results from the oxidation of HE.
[d]These properties are not exploited for the HE-mediated detection of ROS (*see also* **Note 82**).
[e]MDC in solution emits weakly at 425 nm, but its peak is shifted to 498 nm in lipid-rich microenvironments (*see also* **Note 23**).
Abbreviations: CMFDA, 5-chloromethylfluorescein diacetate; CMXRos, chloromethyl-x-rosamine; dH_2O, deionized water; $DiOC_6(3)$, 3,3′ dihexyloxacarbocyanine iodide; DMSO, dimethylsulfoxide; DsRed2, *Discosoma sp*. red fluorescent protein; EthBr, ethidium bromide; FACS, fluorescence-activated cell sorter; FITC, fluorescein isothiocyanate; GFP, green fluorescent protein; HE, hydroethidine; IF, immunofluorescence; LC3, microtubule-associated protein light chain 3; MDC, monodansylcadaverine (5-dimethylaminonaphthalene-1-(*N*-(5-aminopentyl))sulfonamide); mito, mitochondrial targeting sequence from subunit VIII of human cytochrome *c* oxidase; NAO, nonyl acridine orange; PI, propidium iodide; TMRM, tetramethylrhodamine methyl ester.

33. Ponceau S staining solution: 0.1% (w/v) Ponceau S and 5.0% (w/v) acetic acid (Sigma-Aldrich) in dH_2O (or commercially available from Sigma-Aldrich).
34. Protein molecular weight (MW) markers: Precision Plus Protein™ Standard, Dual Color (Bio-Rad).
35. Rinsing buffer: 0.1% Tween-20 in PBS. Storage at RT.
36. Running gel buffer: 1.5 *M* Tris buffer (pH 8.8, from Bio-Rad).
37. Sörensen phosphate buffer (1X, 0.1 *M*, ph 7.3): 23 mL of 0.2 *M* NaH_2PO_4 + 77 mL of 0.2 *M* Na_2HPO_4 + 100 mL dH_2O.
38. Stacking gel buffer: 0.5 *M* Tris buffer (pH 6.8).
39. Transfer buffer (1X): 100 mL 10X Tris/glycine buffer (Bio-Rad) + 200 mL ethanol + 900 mL dH_2O.
40. Transfer cassette: Mini Trans-Blot Cell (Bio-Rad).
41. Transmission electron microscope: Tecnai G2 Spirit (FEI, Eindhoven, The Netherlands).
42. Transparent plastic film (Saran, as used for food preservation).
43. Trichloroacetic acid (TCA), stock solution 10% (w/v) in dH_2O (stored at RT).
44. Uranyl acetate: dissolve 10 g of uranyl acetate dihydrate in 100 mL of methanol (Carlo Erba Reagents); shake or vortex until complete dissolution; store at −20°C.

2.4. Measurement of the Colocalization of Cytoplasmic Organelles with Autophagic Vacuoles

1. 0.1% (w/v) SDS in PBS.
2. 10% FBS (PAA Laboratories GmbH) in PBS.
3. Antibodies employed for immunofluorescence microscopy assessments are listed in **Table 6**.
4. BSA buffer: 3 mg/mL BSA (Sigma-Aldrich) in PBS.
5. Confocal microscope: Zeiss LSM 510 (Carl Zeiss AG, Oberkochen, Germany).
6. Fluorochromes used to measure the colocalization of cytoplasmic organelles with autophagic vacuoles are listed in **Table 5**.

2.5. Measuring Cell Death–Related Parameters

1. Annexin V-FITC kit for the detection of phosphatidylserine externalization (Miltenyi Biotec, Bergisch Gladbach, Germany).
2. Carbonyl cyanide *m*-chlorophenylhydrazone (CCCP, from Sigma-Aldrich), stock solution in ethanol, 10 m*M*, stored at −20°C.
3. Cytofluorometer: FACScan (Becton Dickinson, San Jose, CA) equipped with an argon ion laser emitting at 488 nm.
4. Fluorescent probes used to measure cell death–related parameters are listed in **Table 5**.

Table 6
Antibodies for Immunofluorescence Microscopy

Primary antibody	Specificity	Source organism	Company[a]	Ref.
Anti-AIF internal domain	Polyclonal IgG	Rabbit	Chemicon International	AB 16501
Anti-Calreticulin	Polyclonal IgG	Rabbit	Stressgen Bioreagents	SPA-600D
Anti-Caspase-3a (Asp175)	Polyclonal IgG	Rabbit	Cell Signalling Technology	9661
Anti-cytochrome *c* (clone 6H2.B4)	Monoclonal IgG_1	Mouse	BD Pharmingen	556432
Anti-Hsp60 (clone LK1)	Monoclonal IgG_1	Mouse	Sigma-Aldrich	H4149
Anti-LAMP2	Monoclonal IgG_1	Mouse	Santa Cruz Biotechnology	sc-18822
Secondary antibody	**Label**	**Source organism**	**Company**	**Ref.**
Anti-mouse	Alexa Fluor® 488	Goat	Molecular Probes	A-11001
Anti-mouse	Alexa Fluor® 568	Goat	Molecular Probes	A-11031
Anti-rabbit	Alexa Fluor® 568	Goat	Molecular Probes	A-11036

[a]BD Pharmingen, San Diego, CA; Cell Signalling Technology, Danvers, MA; Chemicon International, Temecula, CA; Molecular Probes-Invitrogen, Carlsbad, CA; Santa Cruz Biotechnology, Santa Cruz, CA; Sigma-Aldrich, St. Louis, MO; Stressgen Bioreagents, Ann Arbor, MI.

3. Methods

Cells that activate the autophagic program, manifest in the accumulation of double-membraned autophagic vesicles in the cytoplasm. These vacuoles can be classified according to their electron density, as assessed by transmission electron microscopy, into early and late AV. Early AV (AV1) contain cytoplasmic portions and/or organelles and exhibit an electron density equivalent to the cytoplasm (AV1). Late or degradative AV (AV2) show evidence of partially digested luminal content and are characterized by increased electron density.

The mere presence of AV in the cytoplasm does not necessarily indicate an increased level of autophagy, since a reduction of the fusion between autophagosomes and lysosomes suffices to promote AV accumulation. Thus, quantitative

methods for the detection of cytoplasmic protein turnover should be employed in addition to AV monitoring, in order to verify augmented levels of autophagy.

3.1. Experimental Modulation of Autophagy

Given its importance in cellular homeostasis and response to stress, it is not surprising that autophagy is a precisely controlled process that is regulated by several (cross-talking) signaling pathways ***(24,25)***. In this context, a major role is played by the mammalian target of rapamycin (mTOR) protein, a serine/threonine kinase implicated in the control of several cellular functions ***(26,27)***. mTOR integrates numerous inputs (including signals from growth factors, insulin, cellular stressors as well as those reporting the availability of nutrients) to stimulate protein synthesis via the phosphorylation of key translation regulators like ribosomal protein S6 kinase (p70SK6) and eukaryotic initiation factor 4E binding protein 1 (eIF4EBP1) ***(28)***. Accordingly, mTOR is a major gatekeeper and inhibitor of autophagy, and may exert its anti-autophagic effects either by promoting protein synthesis or by a direct inhibition of crucial *atg* proteins. Other important regulators of autophagy include class I and class III PI3Ks. The increase in class I PI3K products (like phosphatidylinositol 3,4-bisphospate, i.e., PIP2, and phosphatidylinositol 3,4,5-trisphospate, i.e., PIP3), caused by feeding the cells with synthetic lipids or via by stimulating the interleukin-13 receptor, has been reported to inhibit macroautophagy ***(29)***. Conversely, class III PI3K (hVps34) activates autophagy by interacting with Beclin-1 and plays a crucial role at early stages of autophagosome formation ***(30)***.

3.1.1. Induction of Autophagy

In vitro, several strategies may be employed to induce autophagy (**Fig. 1**). These include: the inhibition of mTOR (e.g., by starvation, by inhibition of the upstream class I PI3K-mediated signaling, or by administration of the mTOR specific inhibitor rapamycin) ***(27,31)***; the inhibition of inositol monophosphatase (IMPase), resulting in a reduction of free inositol and inositol-1,4,5-triphosphate (IP3) levels (e.g. with lithium, L-690,330 or carbamazepine) ***(32)***; the blockade of the IP3 receptor (IP3R) of the endoplasmic reticulum (ER) (e.g., with xestospongin B and C) ***(33)***; the induction of ER stress via the activation of the unfolded protein response (e.g., with tunicamycin, thapsigargin or brefeldin A) ***(34)***; or the induction of oxidative stress (e.g. with H_2O_2) ***(35)***.

1. Wild-type HeLa cells are cultured in appropriate growth medium and passaged when approaching to confluence with trypsin/EDTA to provide new maintenance cultures in 175-cm^2flasks and experimental cultures. The latter are performed

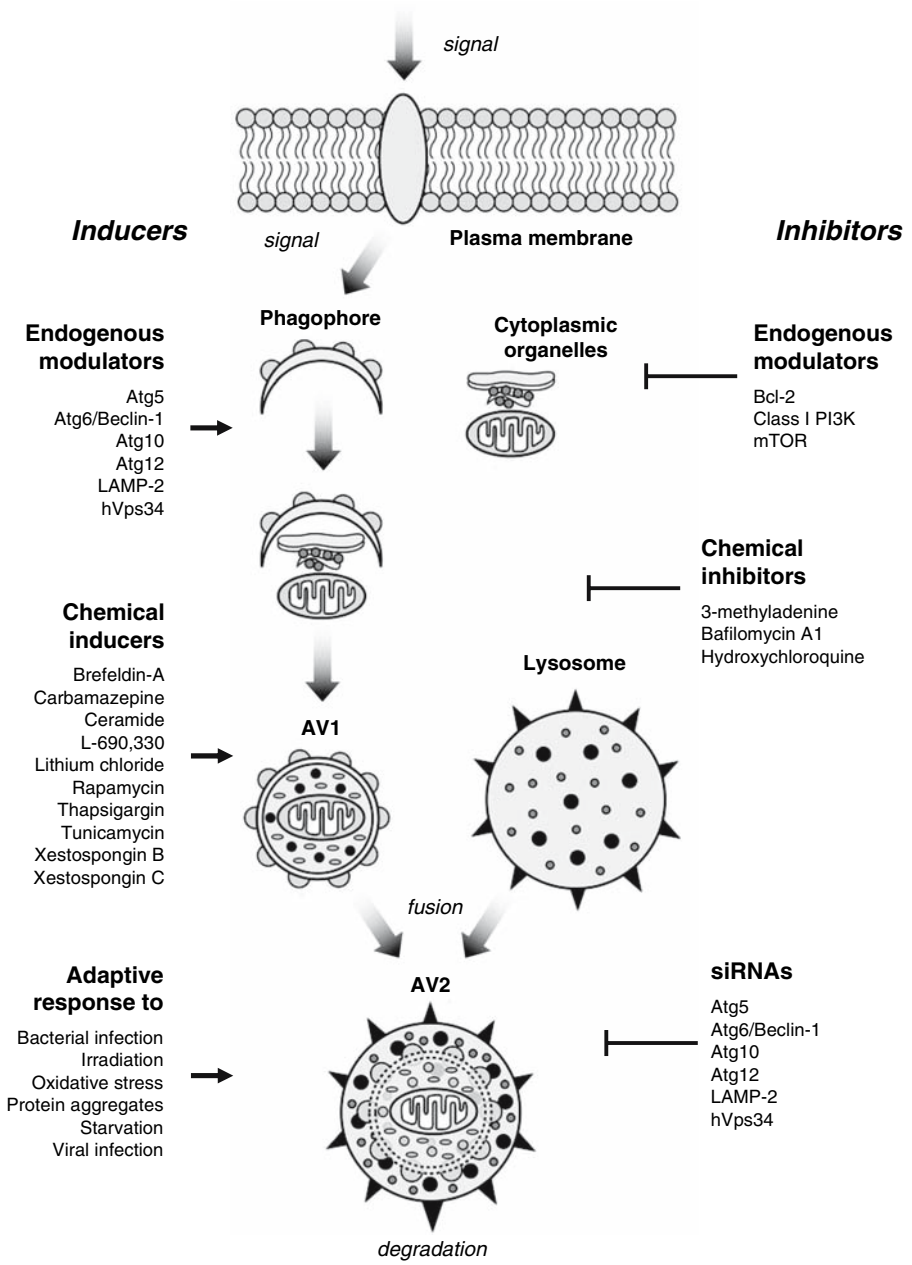

Fig. 1. Overview of the autophagic pathway. The formation of autophagic vacuoles begins with the segregation of portions of cytoplasm and/or cytoplasmic organelles by lipid-rich apparatuses also known as phagophores. This generates immature autophagosomes (AV1), which are doubled-membraned vacuoles in which the luminal content has

either in 12-well plates (100×10^3cells in 1 mL of growth medium) or in 24-well plates in which sterile cover slides have been previously deposited (25×10^3 cells in 0.5 mL of growth medium).

2. Twelve to 24 h after plating, induction of autophagy is performed. To this aim, growth medium is removed by aspiration and cells are washed twice with 1 or 2 mL (in 24- or 12-well plates, respectively) sterile PBS. Then, autophagy inducers (*see* **Table 1**) are administered in growth medium at the appropriate concentration (*see* **Note 1**). Alternatively, growth medium is substituted with 0.5–1 mL of Earle's balanced salt solution (EBSS, nutrient-free [NF] medium). Finally, cells are incubated at 37ºC in 5% CO_2 atmosphere for a variable time frame, depending on the experimental setting (*see* **Note 2**).
3. Finally, autophagic activity and cell death can be monitored as described below (*see* **Subheading 3.2.**).

3.1.2. Inhibition of Autophagy

The cascade of events leading to autophagy can be suppressed at various steps ***(36)*** **(Fig. 1)**, which include: (1) the formation of autophagosomes; (2) the fusion between autophagosomes and lysosomes ***(3,13)***; and (3) the final, lysosomal degradation phase ***(15,37)***. The inhibition of the autophagic process can be achieved by different means, notably (1) chemical inhibitors (*see* **Table 2**) ***(3,13,15)***; (2) transfection-enforced overexpression of inhibitory proteins ***(8)***; and (3) siRNAs targeting essential *atg* gene products (*see* **Table 3**) ***(3,12,30)***.

3-Methyladenine (3-MA) prevents autophagy at the sequestration step by inhibiting the class III PI3K hVps34 ***(29)***. However, the results of experiments in which 3-MA is employed as an autophagy inhibitor should be evaluated cautiously due to the fact that this compound affects many other signaling pathways (by interacting with kinases such as class I PI3K; c-Jun N-terminal

◀

Fig. 1. *(Continued)* not yet been degraded. It is only after the fusion with lysosomes and the acidification of the luminal content that autophagosomes progress to mature, degradation-competent organelles (AV2). Autophagy represents an adaptive response to different stressful conditions (e.g., the depletion of nutrients, bacterial and viral infections, accumulation of misfolded proteins) and can be triggered by pharmacological inducers such as rapamycin, tunicamycin, or xestospongin B. The inhibition of autophagy (which is regulated by several endogenous signalling pathways) can be achieved by molecules like bafilomycin A1 or hydroxychloroquine as well as by genetic manipulations. In the latter case, the siRNA-mediated depletion of proteins essential for autophagy provides a specific tool to suppress the autophagic pathway. Atg, autophagy-specific gene; hVps34, human vacuole protein sorting factor protein 34; LAMP-2, lysosome-associated membrane protein-2; PI3K, phosphatidylinositol-3 kinase; siRNA, small-interfering RNA.

kinase, i.e., JNK; and mitogen-activated protein kinases, i.e., MAPK) ***(29,38)***. Moreover, at the concentration of 10 m*M* (representing the minimal concentration required to block autophagy), 3-MA also inhibits MMP and other catabolic pathways ***(39)***.

Hydroxychloroquine is a lysosomotropic amine, which is clinically used for the treatment of malaria, rheumatoid arthritis, and systemic lupus erythematosus. As do other immunosuppressant drugs, hydroxychloroquine exhibits cytotoxic properties. This agent induces the alkalinization of the lysosomal lumen, thereby inhibiting the fusion between lysosomes with autophagosomes and interfering with the action of lysosomal hydrolases, which function at an acidic pH. At higher concentrations, hydroxychloroquine induces lysosomal membrane permeabilization (LMP), resulting in the potentially lethal leakage of catabolic hydrolases into the cytosol ***(15)***.

Bafilomycin A1 is a specific inhibitor of the vacuolar H^+-ATPase, the proton pump that acidifies the lysosomal lumen ***(37,40)***. Similarly to hydroxychloroquine, bafilomycin A1 prevents the activation of lysosomal hydrolases and interferes with the fusion between autophagosomes and lysosomes ***(13)***, presumably because lysosomal acidification is required for this step.

The intrinsic disadvantage of chemical inhibitors is that they can exert several unwanted side effects due to the fact that none of the currently available molecules is truly specific for autophagy. The siRNA-mediated depletion of proteins essential for the autophagic pathway is characterized by a high degree of specificity. siRNAs targeting hVps34, Beclin-1, Atg5, Atg10, Atg12, and LAMP-2 are now widely employed to suppress autophagy (*see* **Table 3**) ***(3,12,30)***.

3.1.2.1. Chemical Inhibition of Autophagy

1. HeLa cells are maintained in culture and plated as described above (*see* **Subheading 3.1.1.**).
2. Chemical inhibition of autophagy is performed 12–24 h after plating. As for the induction of autophagy, growth medium is removed, cells are washed twice with sterile PBS, then autophagy inhibitors (*see* **Table 2**) are administered at the appropriate concentration (*see* **Note 1**), either in growth medium (negative control condition) or in NF medium (providing a positive control for autophagy induction). Thereafter, cells are cultured at 37ºC in a 5% CO_2 incubator.
3. After a time frame varying according to the specific experimental aim (*see* **Note 2**), autophagic activity can be measured as described below (*see* **Subheading 3.2.**).

3.1.2.2. siRNA-Mediated Inhibition of Autophagy

1. HeLa cells are seeded in 6-well plates (approximately, 200 10^3 cells in 3 mL of growth medium), in order to obtain confluence levels around 60–70% on the next day.

2. If cells have reached appropriate confluence, transfection of siRNA is performed 12–24 h after plating (*see* **Note 3**). For the delivery of siRNAs to adherent cells, liposome-based transfection is employed. To this aim, 200 nmol of siRNA (final concentration in wells = 100 n*M*) are diluted in 180 µL of Opti-MEM® and 4 µL of Oligofectamine™ transfection reagent (Oligofectamine™) are gently mixed with 16 µL of Opti-MEM®. After a first incubation of 5–10 min, the diluted siRNAs and the diluted Oligofectamine™ solution are combined, gently mixed, and incubated for additional 20 min to allow for the formation of Oligofectamine™:siRNA transfection complexes (*see* **Notes 4** and **5**).
3. Before the addition of the complexes to the cells, growth medium is replaced by 1.8 mL of fresh medium without serum (*see* **Notes 6** and **7**). Then, 200 µL of the solution containing Oligofectamine™:siRNA complexes are added to each well, and plates are incubated at 37ºC in 5% CO_2 atmosphere for 4 h.
4. Four hours after transfection, 220 µL of FBS should be added to each well to restore the final concentration of 10% (as in complete growth medium).
5. Twelve to 24 h after transfection, cells can be trypsinized (500 µL of Trypsin/EDTA per well) and seeded in 12- or 24-well plates, according to the specific experimental settings (*see* **Notes 8–10**).
6. After the time required for the siRNA-mediated downregulation of the target protein (*see* **Note 8**), the desired stimuli can be administered to the cells in which the autophagic pathway has been suppressed by genetic techniques.
7. Finally, following another incubation at 37ºC in 5% CO_2 atmosphere (the duration depends again on the specific experimental conditions), autophagy can be assessed as described below (*see* **Subheading 3.2.**).

3.2. Measuring Autophagy

At present, multiple techniques are available for the quantification of autophagy and the identification of AV. **Table 7** summarizes these methods, by providing also the main advantages and drawbacks of each.

3.2.1. Electron Microscopy

1. 2×10^6cells are cultured in 100 × 20 mm culture dishes.
2. After the treatment with the desired stimuli, cells are fixed for 1 h at 4°C in 1.6% glutaraldehyde in 0.1 *M* Sörensen phosphate buffer (pH 7.3) and washed once with PBS.
3. Cells are then re-fixed in aqueous 2% osmium tetroxide and finally embedded in Epon® epoxy resin, until imaging.
4. Examination is performed at 80 kV under a transmission electron microscope, on ultrathin sections (80 nm) stained with 0.1% lead citrate and 10% uranyl acetate.

Once the images are obtained, the number of type I and type II AV can be quantified on a per-cell basis (*see* **Fig. 2**). In addition, AV volume can be evaluated by morphometric methods.

Table 7
Methods for the Detection of Autophagy

Method	Advantages	Drawbacks
Electron microscopy	Direct observation of the AV	Skill requiring, laborious
	Quantitative (n° of AV per cell, ratio between their surface/volume and that of the cell)	Prone to subjective interpretations (e.g., swollen organelles may be mistaken for AV)
	Differentiates between AV1 and AV2	Scarcely representative of the overall sample (few cells examined)
	Immunoelectron microscopy approaches enable the specific labeling of AV	
LC3-GFP aggregation	Rather specific	Weaker signal from AV2 than from AV1
	Allows for the quantification of AV per cell	Possibility of false-negative and false-positive results
	Can be performed on histological sections	
	Can be coupled to other stainings for co-localization studies	Low amounts of aggregates are prone to misinterpretations, due to basal levels of ongoing autophagy
Bulk degradation of long-lived proteins	Specifically measures turnover of long-lived proteins	Not specific for autophagy nor for lysosomal proteolysis
	TCA-precipitated radioactivity can be used to estimate the intracellular amount of radiolabeled proteins	Excess unlabeled amino acids administered during the chase step may inhibit autophagy
		Not applicable if fusion of AV and lysosomes is interrupted
MDC staining	Stains AV due to ion trapping in acidic compartments and to increased relative fluorescence in hydrophobic milieus	Rather unspecific: stains only acidic vacuoles of the autophagic pathway (AV2), but several other acidic compartments of cells
	Can be used in vivo without construction of transgenic animals	Cannot be used alone for the detection/quantification of autophagy

CellTracker™ Green staining	Useful in double staining techniques to distinguish AV from other vacuolar compartments	Totally unspecific (it detects all vacuolar compartments)
		Cannot be used alone to assess autophagy
LC3-I to LC3-II conversion	Specific (autophagy never observed in the absence of LC3-I to LC3-II conversion and LC3-II incorporation in AV)	Provides an estimate of the instantaneous levels of autophagy rather than of the overall autophagic flux (due to relatively short lifetime of AV)
	LC3-II/LC3-I ratio correlates with the extent of autophagic activity	Antibodies against LC3 display higher affinity for LC3-II, resulting in overestimation of the corresponding band
		Possibility of false-positive results

Abbreviations: AV, autophagic vacuoles; GFP, green fluorescent protein; LC3, microtubule-associated protein light chain 3; MDC, monodansylcadaverine.

3.2.2. LC3-GFP Aggregation

1. HeLa cells (25×10^3 in 0.5 mL growth medium) are seeded in 24-well plates in which sterile cover slips have been previously deposited.
2. Twelve to 24 h later, cells are transfected with a plasmid coding for the autophagosome marker LC3 fused with green fluorescence protein (GFP) ***(6)***, according to the following protocol. 4 µg of plasmid are diluted in 200 µL of Opti-MEM®, at the same time as 5 µL of Lipofectamine™ are gently mixed with 200 µL Opti-MEM®. After a first incubation of 5–10 min, the diluted plasmid solution and diluted Lipofectamine™ solution are gently mixed and incubated for another 20 min to promote the formation of Lipofectamine™:plasmid complexes (*see* **Notes 4** and **5**).
3. Thereafter, 30 µL of solution containing the Lipofectamine™:plasmid complexes are added to each well, in which medium had been previously replaced with 500 µL of serum-free growth medium. Plates are then incubated at 37ºC in 5% CO_2 atmosphere for 4 h before 60 µL of FBS are added to restore the final FBS concentration of 10% (as in complete growth medium) (*see* **Note 6**).
4. Cells are cultured for 24 h, or until they start to express the LC3-GFP fusion protein, prior to treatment with the desired stimuli (*see* **Notes 11** and **12**).
5. At the end of stimulation, growth medium is removed, cells are washed twice with PBS and fixed in 400 µL of fixative solution for 30 min at RT (*see* **Notes 13–16**).

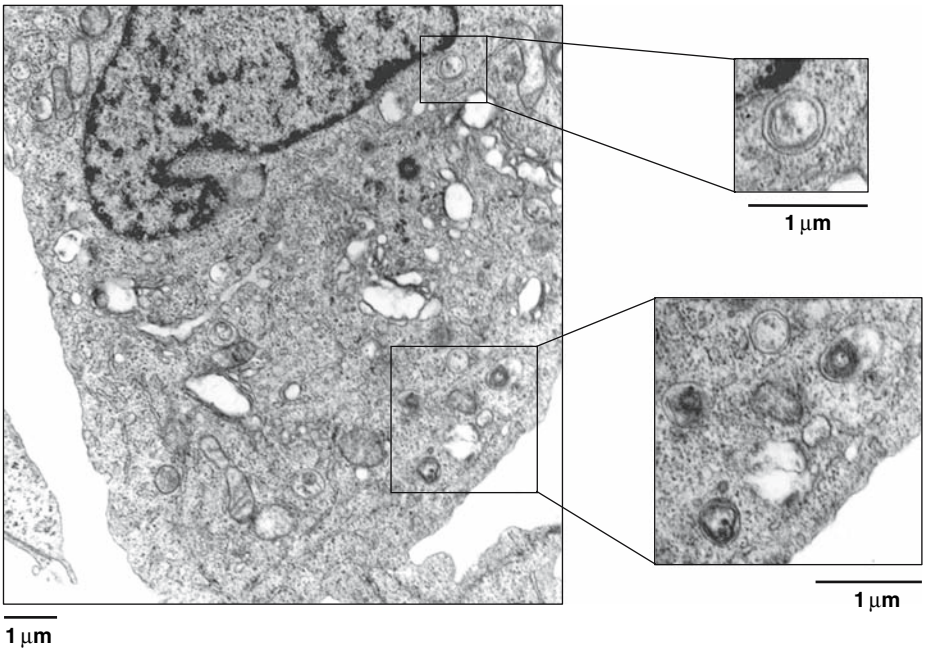

Fig. 2. Ultrastructural features of autophagy. HeLa cells were treated with 2.5 μ*M* tunicamycin for 6 h and processed for electron microscopy, as described in **Subheading 3.2.1**. The induction of autophagy is witnessed by massive vacuolization of the cytoplasm. In the same cells, immature autophagic vacuoles characterized by an electron density equivalent to the cytoplasm coexist with late vesicles, in which catabolic processes have been already started (characterized by an increased electron density). Black bars report picture scale.

6. Fixative solution is removed, cells are washed three times with PBS, and nuclear counterstaining is performed by the addition of 2 μ*M* Hoechst 33342 in PBS (200 μL per well) for 10 min (*see* **Note 17**).
7. The cover slips are mounted onto slides using Fluoromount-G™ mounting medium prior to examination in a fluorescence microscope. For the visualization of LC3-GFP, cells should be examined using an oil immersion objective (50–65× magnification). Suitable excitation and emission filters should be selected according to the following absorption and emission peaks: 488/507 nm for LC3-GFP and 352/461 nm for Hoechst 33342 (*see* **Note 18**). The LC3-GFP fusion protein redistributes from a diffuse (cytoplasmic and nuclear) to a vacuolar, punctuate (exclusively cytoplasmic) pattern when AV are formed (*see* **Fig. 3** and **Note 19**)

3.2.3. Bulk Degradation of Long-Lived Proteins

1. HeLa cells (400×10^3 in 2.5 mL growth medium) are plated in 6-well plates.

2. Forty-eight hours later, growth medium is replaced by 0.2 μCi/mL L-[U-^{14}C]valine (*see* **Note 20**) in complete medium. Plates are then incubated at 37°C in 5% CO_2 atmosphere for 24 h.
3. At the end of the radiolabeling period, cells are washed three times with PBS (to remove unincorporated radioisotopes), and incubated with 10 m*M* unlabeled L-valine in complete growth medium (2–2.5 mL) for 1 h (prechase period) (*see* **Note 21**).
4. After the prechase step, the culture medium is again replaced by fresh medium containing 10 m*M* unlabeled valine in the presence or absence of an autophagy inhibitor (e.g., 3-MA) (*see* **Note 22**). Cells are then incubated with the desired stimuli for 4–12 h (chase period).
5. After the chase step, supernatant is collected and proteins from the medium and from cells are precipitated separately with 10% (w/v) TCA (overnight, 4°C).
6. Thereafter, TCA-precipitated fractions are centrifuged (600*g*, 20 min, RT) and redissolved in 1 mL of 0.2 *N* NaOH. Finally, radioactivity is determined by liquid scintillation counting.
7. The rate of degradation of long-lived proteins can be calculated by determining the ratio of TCA-precipitated radioactivity recovered from the medium to the sum of TCA-precipitated radioactivity from the medium and cells:

$$\%\text{Proteolysis}(h^{-1}) = R_m/(R_c + R_m)$$

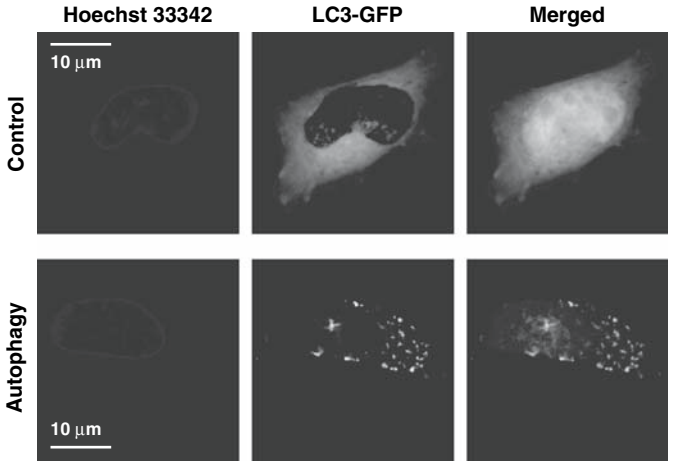

Fig. 3. Detection of autophagy by the LC3-GFP aggregation technique. HeLa cells transfected with a plasmid encoding the LC3-GFP fusion protein (as described in **Subheading 3.2.2.**) were left untreated (Control) or treated with 2.5 μ*M* tunicamycin for 6 h (Autophagy). Thereafter, cells were processed for fluorescence microscopy examination, as detailed in **Subheading 3.2.2**. In untreated cells LC3-GFP exhibits a diffuse cytoplasmic signal. When autophagy is induced, LC3-GFP chimeric proteins aggregate in autophagic vacuoles, leading to a punctuate cytoplasmic staining. As confirmed by Hoechst 33342 counterstaining, LC3-GFP is not found in the nucleus.

where R_m is TCA-precipitated radioactivity from medium and R_c is TCA-precipitated radioactivity from cells.

3.2.4. Monodansylcadaverine (MDC) Staining of Autophagic Vacuoles

1. HeLa cells (25×10^3 in 0.5 mL of growth medium) are seeded in 24-well plates where sterile cover slips have been previously dropped.
2. Following the desired stimuli for the induction or inhibition of autophagy, AV are labeled with 50 μ*M* MDC in growth medium (0.5 mL) for 30 min at 37°C.
3. Then, cells are washed three times with PBS and fixed in 400 μL of 4% PFA (*see* **Notes 13** and **14**) for 30 min at RT. After fixation, PFA is removed and cells are washed once with PBS. Finally, cover slips are mounted as described above (*see* **Subheading 3.2.2., step 7**).
4. As for LC3-GFP staining, the assessment of AV is performed by fluorescence microscopy, at magnifications of 50–65×. Usually, MDC is observed with a 335(380)/525 nm (excitation/emission) filter set (*see* **Note 23**). The percentage of cells with punctuate structures should be assessed among a sample of statistical relevance (*see* **Notes 19** and **24**).

3.2.5. CellTracker™ Green (CMFDA) Staining

1. 25×10^3 HeLa cells are cultured in 24-well plates with sterile coverslips (0.5 mL growth medium).
2. After the stimulation or inhibition of autophagy, cells are stained with 1 μ*M* CMFDA at 37ºC in a 5% CO_2 incubator for 30 min.
3. Then, cells can be fixed and counterstained with Hoechst 33342 as described above (*see* **Subheading 3.2.2., steps 5–7**, and **Notes 13–17**).
4. CMFDA staining is routinely examined in fluorescence microscopy with a 488/525 (excitation/emission) filter set (*see* **Note 25**).
5. With this technique, AV vacuoles appear as "holes" within a diffuse green cytoplasmic fluorescence. The percentage of cells bearing at least one discernable cytoplasmic vacuole should be determined (*see* **Note 19**).

3.2.6. LC3-I–to–LC3-II Conversion by Immunoblotting

3.2.6.1. Preparation of Samples

1. HeLa cells (5×10^5in 3 mL of growth medium) are cultured in 6-well plates.
2. Following the desired treatments to induce or suppress autophagy, cells are collected by trypsinization, washed once in cold (4°C) PBS and pelleted (300–500*g*, 5 min, 4°C) (*see* **Note 26**).
3. Supernatant is discarded, and pellets are lysed in 30–50 μL of lysis buffer (*see* **Notes 27** and **28**).
4. The protein concentration of lysates is determined by means of the Bio-Rad DC Protein Assay, following the manufacturer's instructions (*see* **Note 29**).

5. Then, 4–6 µL of 5X loading buffer are added to 20–80 µg of proteins from each lysate, and the final volume is adjusted to 20–30 µL with dH_2O (*see* **Notes 30** and **31**).
6. Finally, samples are incubated for 5 min at 100°C. After cooling to RT, samples are ready for separation by sodium dodecylsulfate–polyacrylamide gel electrophoresis (SDS-PAGE) (*see* **Note 32**).

3.2.6.2. SDS-PAGE

1. These instructions assume the use of a BioRad mini-PROTEAN 3 system for gel electrophoresis. The protocol is easily adaptable to other formats.
2. A 1.0-mm-thick, 15% running gel (*see* **Note 33**) is prepared by mixing 1.8 mL of 40% acrylamide:*N-N'*-methylenediacrylamide (29/1) solution (*see* **Note 34**), 1.25 mL of running gel buffer (pH 8.8), 1.8 mL of dH_2O, 50 µL of 10% SDS, 10 µL of TEMED (*see* **Notes 35** and **36**), and 26 µL of 10% APS (*see* **Notes 37** and **38**). Immediately after the addition of APS (to avoid polymerization in tube; *see* **Notes 39** and **40**), gel should be poured into preassembled glasses up to approximately two thirds of their height (*see* **Notes 41** and **42**).
3. Quickly following, overlay gel with isopropanol (*see* **Note 43**) to ensure a flat surface and exclude air.
4. After the polymerization (*see* **Note 44**), isopropanol is poured off and the top of the gel is washed with dH_2O.
5. The stacking gel (*see* **Note 45**) is prepared by mixing 250 µL of 40% acrylamide/bisacrylamide (29/1) solution (*see* **Note 34**), 625 µL of stacking gel buffer (pH 6.8), 1.6 mL of dH_2O, 50 µL of 10% SDS, 9 µL of TEMED (*see* **Notes 35** and **36**), and 15 µL of APS (*see* **Notes 37** and **38**). Rapidly following the addition of APS, the stacking gel is poured on top of the polymerized running gel and the comb for the creation of wells is inserted (*see* **Notes 38** and **46**).
6. Once the stacking gel is polymerized, the comb is gently removed and the gel unit is moved to the cell for separation. Upper and lower chambers of the gel unit are filled with migration buffer (1X) (*see* **Note 47**), which is used also to gently wash sample wells.
7. At this stage, each well is loaded with a sample prepared as described above (*see* **Subheading 3.2.6.1.**). One well is reserved for protein MW markers (*see* **Note 48**).
8. Finally, the gel unit is connected to power supply and the proteins are separated in constant-field mode (*see* **Note 49**). The run should be arrested when MW markers are separated throughout entire height of the gel (*see* **Note 50**).

3.2.6.3. Immunoblotting (Western Blotting)

1. Two sponges and four sheets of filter paper of approximately the same size as the running gel are incubated in transfer buffer (1X) for 1–2 min at RT.
2. One nitrocellulose membrane of approximately the same size of the running gel is activated by incubation in dH_2O for 5–10 min at RT, then equilibrated in transfer buffer.

3. The gel unit is disconnected from the power supply and disassembled. The stacking gel is discarded.
4. The transfer "sandwich" is prepared by overlaying the following components (*see* **Note 51**): one sponge, two sheets of Whatmann paper, the nitrocellulose membrane, the running gel, two sheets of Whatmann paper, one sponge.
5. The "sandwich" is placed in a transfer cassette (*see* **Note 52**), which is subsequently inserted into the transfer apparatus. Special attention should be paid in the orientation of the cassette to ensure that the nitrocellulose membrane is placed between the gel and the anode (*see* **Note 53**).
6. To control temperature, an ice block is placed next to the transfer cassette (*see* **Note 54**). The cell is then completely filled with transfer buffer (1X). A magnetic stir-bar is placed in the cell to help in maintaining a homogeneous solution and temperature.
7. The power supply is activated, and the transfer is accomplished at the constant voltage of 90 V for 2 h (*see* **Notes 55** and **56**).
8. Once the transfer is complete, the cassette is disassembled. Sponges and sheets are removed (*see* **Note 57**). The colored MW markers should be visible on the nitrocellulose membrane.
9. The bound proteins can be visualized by a rapid incubation with Ponceau S staining solution (*see* **Note 58**). Prior to the blocking, Ponceau S should be removed by rinsing the membrane with PBS or dH_2O.
10. To block unspecific binding sites, the nitrocellulose membrane is incubated on a rocking platform in 10 mL of blocking buffer (45–40 min, RT).
11. Blocking buffer is discarded, membrane is quickly rinsed in rinsing buffer and a 1/200 dilution of rabbit anti-LC3 polyclonal antibody (in 5–10 mL of blocking buffer) is added. Incubation with the primary antibody can be performed either at RT for 2 h or at 4°C overnight, in both cases on the rocking platform.
12. Once the primary antibody is removed, the membrane is washed three times with rinsing buffer (5 min, RT).
13. Upon washing, membrane is incubated for 1 h at RT (on the rocking platform) with a freshly prepared 1/5000 dilution in blocking buffer of goat anti-rabbit horseradish peroxidase (HRP)–labeled secondary antibody.
14. Secondary antibody solution is removed and the membrane is again washed three times (5 min, RT) with rinsing buffer.
15. The membrane is overlaid with 2 mL of chemiluminescent substrate for 1 min (*see* **Note 59**). Then, chemiluminescent substrate is removed and the membrane is moved to an x-ray film cassette.
16. In the dark room, a photographic film (*see* **Note 60**) is exposed to the membrane for a suitable time, typically 3 or 4 min (*see* **Notes 61** and **62**).
17. Finally, exposed films are developed in a common table-top film processor.
18. To ensure equal loading of the samples onto the gel (thus comparability of the bands), membrane can be dehybridized from bound antibodies by incubation in dehybridizing buffer for 15 min at RT, followed by one wash in rinsing buffer and by repetition of the **steps 10–17** with the following antibodies:

- Primary antibody: mouse anti-glyceraldehyde-3-phosphate dehydrogenase (GAPDH) monoclonal antibody (*see* **Note 63**), 1/10000 in 10 mL of blocking buffer, 1 h, RT.
- Secondary antibody: goat anti-mouse HRP-labeled secondary antibody, 1/5000 in 10 mL of blocking buffer, 1 h, RT.

LC3-II is the posttranslationally processed form of LC3, which localizes to autophagosomes and autophagolysosomes during autophagy ***(6)***. Under nonautophagic conditions, the AV marker LC3 appears as a single band of approximately 18 kDa, corresponding to LC3-I, the uncleaved isoform. Following the induction of autophagy, LC3-II (the cleaved isoform of LC3) can be visualized as an additional band with a slightly higher electrophoretic mobility than LC3-I (approximately 16 kDa).

3.3. Methods to Measure the Colocalization of Cytoplasmic Organelles with Autophagic Vacuoles

3.3.1. Lysosomes

Lysosomes are acidic vesicles that participate in the degradation of extracellular macromolecules that are taken up via endocytosis, micropinocytosis, or phagocytosis. Lysosome are also implicated in the catabolism of cytoplasmic components through autophagy ***(36)***. The most abundant proteins found in lysosomal membranes are the lysosome-associated membrane proteins 1 and 2 (LAMP-1 and -2), which together constitute almost 50% of all lysosomal membrane proteins. To study the fusion between AV and lysosomes, colocalization experiments can be performed according to different staining techniques.

3.3.1.1. LAMP-2 Immunofluorescence Staining

1. HeLa cells are cultured in 24-well plates, transfected with the LC3-GFP plasmid and treated as described above (*see* **Subheading 3.2.2., steps 1–4**, and **Notes 4–6, 11,** and **12**).
2. After the desired stimulation, growth medium is discarded, cells are washed twice with PBS, and incubated with fixative solution for 30 min at RT. Thereafter, cells are rinsed an additional three times with PBS (*see* **Notes 13–16**).
3. Incubation for 10 min (RT) in 0.1% SDS is used to permeabilize cells. Then, cells are rinsed three times with PBS and nonspecific binding sites are blocked by incubating the samples for 20 min at RT with 10% FBS (in PBS). Subsequently, cells are again washed once with PBS.
4. For staining, cells are incubated with the mouse anti-LAMP-2 monoclonal primary antibody (1/100 dilution in 500 µL of BSA buffer). Incubation can be performed either at RT for 1 h or at 4°C overnight.

5. Primary antibody solution is removed, cells are washed three times with PBS and incubated for 1 h at RT with the Alexa Fluor® 568-conjugated secondary antibody (1/300 dilution in 500 µL of BSA buffer) (*see* **Note 64**).
6. Finally, BSA buffer is discarded, stained cells are rinsed three times with PBS and cover slips are mounted as described above (*see* **Subheading 3.2.2., step 7**).
7. To determine the colocalization between AV and lysosomes, confocal fluorescence microscopy should be performed at 63X magnification (*see* **Note 65**) on a device equipped with a dual FITC-Texas Red filter combination (*see* **Notes 66** and **67**).
8. Percentage of colocalization is quantified by software-assisted analysis of green, red, and green-red merged images (*see* **Note 68**).

3.3.1.2. LysoTracker® Probes

LysoTracker® probes are fluorescent acidotropic, lysosomotropic, readily cell-permeant fluorochromes for labeling and tracking acidic compartments in living cells. These molecules accumulate in lysosomes and autophagosomes (as well as in other acidic subcellular compartments) due to their chemical character of weak basic amines. Since such probes are not specific for autophagosomes, they cannot be used alone to assess and/or quantify autophagy ***(41)***.

LysoTracker® probes exist in several variants, which exhibit distinct excitation and emission spectra, to facilitate double or triple stainings. For instance, when AV are labeled with LC3-GFP (emitting in green), colocalization of AV and lysosomes can be visualized with LysoTracker® Blue or Red.

1. 25×10^3 HeLa cells are cultured in 24-well plates, transfected with the LC3-GFP plasmid, and treated as described above (*see* **Subheading 3.2.2., steps 1–4** and **Notes 4– 6, 11,** and **12**).
2. At the end of the desired treatments, growth medium is removed, cells are washed twice with PBS, then prewarmed medium containing the selected LysoTracker® probe (e.g., LysoTracker® Red) at the final concentration of 50–75 n*M* is added. Staining is performed at 37°C, in 5% CO_2 atmosphere, for a minimal time of 30 min (*see* **Note 69**).
3. The staining solution is removed, cells are washed once with PBS, and cover slips are mounted as described above (*see* **Subheading 3.2.2., step 7**).
4. The cells should be observed using a confocal microscope equipped with a 63X objective (*see* **Notes 65** and **66**). A dual FITC-Texas Red filter combination is appropriate to visualize both the LC3-GFP fusion protein and LysoTracker® Red (*see* **Note 67**).
5. To determine the percentage of colocalization, software-assisted analysis of green, red, and red-green merged images is performed (*see* **Note 68**).

3.3.2. Mitochondria

Mitochondria are vital organelles for cellular metabolism and bioenergetics, but they are also the major regulators of cell death. Indeed, in many (if not all)

paradigms of apoptosis, MMP represents the point of no return in the cascade of events that ultimately leads to the cell's demise ***(42)***. MMP results in the leakage of potentially toxic proteins from the mitochondrial intermembrane space (IMS) into the cytosol. For instance, while cytochrome *c* (Cyt *c*) in the IMS has vital functions (by acting as an electron shuttle in oxidative phosphorylation), it participates in the activation of caspases when it is released from mitochondria ***(43)***. In addition, mitochondria play a role in stress responses and can produce reactive oxygen species (ROS) when damaged ***(44,45)***. Selective degradation of mitochondria by autophagy is also known as "mitophagy" and is thought to be promoted by their functional impairment and/or by MMP. Mitophagy may ensure the removal of damaged and potentially dangerous mitochondria, thus acting as a quality control mechanism ***(46)***.

3.3.2.1. Transfection with pDsRed2-mito

pDsRed2-mito is a mammalian expression vector that encodes a fusion of *Discosoma sp*. red fluorescent protein (DsRed2) ***(47)*** and the mitochondrial targeting sequence from subunit VIII of human cytochrome *c* oxidase (mito) ***(48,49)***. Upon expression, this chimeric protein readily localizes to the mitochondrial matrix, thus allowing for the visualization and tracking of mitochondria. The simultaneous detection of AV (with LC3-GFP) and mitochondria (with DsRed2-mito) provides a means to estimate the degree of mitophagy in cells.

1. HeLa cells are seeded in 24-well plates, as described above (*see* **Subheading 3.2.2., step 1**).
2. Twelve to 24 h after seeding, cells are co-transfected with LC3-GFP and pDsRed2-mito plasmids. For the transient transfection of cells with two plasmids, the same protocol reported above (*see* **Subheading 3.2.2., steps 2–4**, and **Notes 4–6, 11,** and **12**) is applied. Importantly, the ratio between the total amount of plasmid DNA and Lipofectamine™ has to be maintained, so 2 μg of LC3-GFP plasmid and 2 μg of pDsRed2-mito should be employed.
3. Following the desired treatments, cells are washed once with PBS and cover slips are mounted as detailed above (*see* **Subheading 3.2.2., step 7**).
4. Confocal fluorescence microscopy is then performed at 63X magnification (*see* **Notes 65** and **66**). The LC3-GFP and DsRed2-mito fusion proteins can be appropriately visualized by employing a dual FITC-Texas Red filter combination (*see* **Note 67**).
5. The degree of colocalization between green and red fluorescence is determined as described above (*see* **Subheading 3.3.1.1.** and **Note 68**).

3.3.2.2. MitoTracker® Probes

MitoTracker® probes are cell permeant, mitochondrion-selective, fluorescent stains that are concentrated by active mitochondria and well retained during

fixation ***(50)***. This latter feature (which is not shared by conventional mitochondrial probes such as rhodamine 123 or tetramethylrosamine) seems to depend on the presence of a mildly thiol-reactive chloromethyl moiety. As for LysoTracker® probes, several variants of MitoTracker® probes exist for use in double or triple staining protocols (e.g., LC3-GFP and MitoTracker® Red to determine the colocalization of AV and mitochondria).

1. For colocalization studies of AV marked with LC3-GFP fusion protein and mitochondria stained with MitoTracker® Red CMXRos, the same protocol described above for LysoTracker® Red (*see* **Subheading 3.3.1.2., steps 1–3**, and **Notes 4–6, 11, 12, and 69**) is followed.
2. In contrast to LysoTracker® probes, MitoTracker® probes should be employed at the final concentration of 150 n*M*.
3. Confocal microscopy assessments are performed as detailed above (*see* **Subheading 3.3.1.2.,– steps 4** and **5**, and **Notes 65–68**).

3.3.2.3. Heat Shock 60 kDa Protein (Hsp60) Immunofluorescence Staining

In eukaryotes, Hsp60 is mainly localized to the mitochondrial matrix and is not released during cells death. Thus, it has been widely employed as a specific marker of mitochondria ***(51,52)***.

1. HeLa cells are cultured, transfected, treated, permeabilized, and fixed as described above for LAMP-2 staining (*see* **Subheading 3.3.1.1., steps 1–3**, and **Notes 4–6, 11–16**).
2. For staining, cells are incubated with the mouse anti-Hsp60 monoclonal primary antibody (1/100 dilution in 500 µL of BSA buffer). Incubation can be performed either at RT for 1 h or at 4°C overnight.
3. Subsequent washing, incubation with the Alexa Fluor® 568-conjugated secondary antibody, mounting and confocal microscopy determinations are carried out as described above (*see* **Subheading 3.3.1.1., steps 5–8** and **Notes 64–68**).

3.3.3. Endoplasmic Reticulum

The ER is a network of or interconnected tubules, vesicles, and sacs involved in multiple processes, including the regulation of cytosolic calcium concentrations. Several studies suggest that the membranes of AV originate from ER. Calreticulin is the most prominent calcium-binding protein found in the ER lumen ***(53)*** and can be used as a marker in AV-ER colocalization experiments.

1. HeLa cells are grown, transfected, treated, permeabilized, and fixed as described above for LAMP-2 staining (*see* **Subheading 3.3.1.1., steps 1–3** and **Notes 4–6, 11–16**).

2. For staining, cells are incubated with the rabbit anti-calreticulin polyclonal primary antibody (1/100 dilution in 500 µL of BSA buffer). Incubation can be performed either at RT for 1 h or at 4°C overnight.
3. Subsequent washing, staining with the Alexa Fluor® 568-conjugated secondary antibody, mounting, and confocal microscopy determinations are carried out as described above (*see* **Subheading 3.3.1.1., steps 5–8** and **Notes 64–68**).

3.4. Methods for Measuring Cell Death–Related Parameters

Most cell death in vertebrates proceeds via the intrinsic, mitochondrial pathway of apoptosis ***(54)***. In several models of cell death, MMP is considered as the point of no return in the pro-apoptotic cascade of events ***(42)***. MMP may result from the activity of pro-apoptotic members of the Bcl-2 family (such as Bax, Bak, and BH3-only proteins like Bid) ***(55,56)*** or from the opening of a multiprotein complex, the permeability transition pore complex (PTPC) ***(57,58)***. The sudden increase in permeability of the mitochondrial inner membrane (IM) that derives from PTPC opening (a process known as mitochondrial permeability transition, MPT) leads to dissipation of the mitochondrial transmembrane potential$\Delta\Psi_m$ and eventually to the rupture of the mitochondrial outer membrane (OM) ***(42)***. Irrespective of its initiation (be it mediated by Bcl-2 pro-apoptotic proteins or by opening of the PTPC), MMP leads to the functional impairment of mitochondria and to the release of IMS proteins into the cytosol. These include caspase activators like Cyt *c* ***(43,59)***, Omi/HtrA2 (Omi stress-regulated endoprotease/high temperature requirement protein A 2) ***(60)*** and Smac/DIABLO (second mitochondria-derived activator of caspase/direct IAP binding protein with a low pI) ***(61,62)***, as well as caspase-independent cell death effectors such as apoptosis-inducing factor (AIF) ***(63,64)*** and endonuclease G (EndoG) ***(65)***.

The assessment of early mitochondrial alterations allows for to identification of cells that are committed to death but have not yet displayed an apoptotic phenotype. The $\Delta\Psi_m$ (providing direct indications on the IM permeability status) can be assessed by means of cationic fluorescent probes ***(66)***. Such lipophilic dyes (e.g., $DiOC_6(3)$, TMRM) accumulate in mitochondria driven by $\Delta\Psi_m$, according to the Nernst equation, and can be used in situ for microscopic assessments of $\Delta\Psi_m$ as well as in cytofluorometric-based procedures for $\Delta\Psi_m$ quantification ***(52)***.

OM permeabilization can be assessed by the detection of IMS proteins (e.g., Cyt *c*, AIF) in the cytosol. This can be achieved by immunoblotting subcellular fractions with antibodies against Cyt *c* or AIF, or by in situ immunofluorescence microscopy on fixed and permeabilized cells ***(51,67,68)***. As an alternative, cells can be transfected with cDNA constructs encoding IMS proteins fused to a GFP moiety ***(69,70)***. Such chimeric proteins are targeted to IMS as their

normal counterparts. Upon apoptosis stimulation, videomicroscopy permits to follow the redistribution of GFP-tagged proteins from IMS to other subcellular compartments in real time. Among these techniques, immunofluorescence microscopy seems the most appropriate to detect the release of IMS protein, since it provides more accurate information on their redistribution than subcellular fractionation followed by immunoblotting, and it is not associated with the technical requirements of videomicroscopy ***(52)***.

One of the classical hallmarks of apoptosis is the externalization of phosphatidylserine (PS) and phosphatidylethanolamine (PE) ***(71,72)***. In normal conditions, these phospholipids are sequestered on the cytoplasmic leaflet of the plasma membrane, but they translocate to the outer leaflet upon apoptosis induction. Fluorescent Annexin V that specifically binds to PS exposed on the extracytoplasmic side of the plasma membrane can be used to identify apoptotic cells.

Following MMP, mitochondrial uncoupling results in enhanced generation of ROS. This alteration may be quantified (in association with other mitochondrial parameters like the $\Delta\Psi_m$) by means of cytofluorometric techniques. For instance, the nonfluorescent probe hydroethidine (HE) is oxidized by ROS to ethidium bromide (EthBr), which emits red fluorescence ***(73)***. In particular, HE is more sensitive to superoxide anion than 2′,7′-dichlorofluorescein diacetate, which preferentially measures H_2O_2 formation ***(45,73,74)***. Alternatively, ROS-induced damage of mitochondria can be determined indirectly, by assessing the oxidation state of cardiolipin, a lipid restricted to the IM. This may be achieved with nonyl acridine orange (NAO), a fluorochrome that specifically interacts with nonoxidized, intact cardiolipin ***(75)***. Consequently, a reduction in NAO fluorescence is an indicator of ROS-mediated cardiolipin oxidation.

Downstream MMP, the activation of the caspase cascade is frequently associated with the onset of apoptotic cell death ***(42,54)***. However, caspase-independent routes to death have been reported in several models of apoptosis ***(76)***. Moreover, caspase activation occurs in several nonapoptotic scenarios ***(77)***. As it stands, the detection of activated caspases cannot be used alone to assess apoptosis, but it may provide a useful complementary assay to other techniques. Among the various caspases that execute the apoptotic program, a prominent one is caspase-3 ***(78)***. Hence, detection of the large fragment (17/19 kDa) of active caspase-3 (caspase-3a), resulting from the caspase-9–mediated cleavage adjacent to Asp175, is commonly considered as an indicator of apoptosis induction.

The integrity of plasma membrane represents a central difference between apoptosis and necrosis. During primary necrosis, the generalized swelling of the cell and of cytoplasmic organelles results in the early breakdown of plasma membrane. On the contrary, plasma membrane integrity is maintained until

the late stages of apoptosis, before secondary necrosis occurs ***(22)***. Thus, the vital dye propidium iodide (PI, emitting in red), which cannot enter living cells nor cells undergoing apoptosis, can be used to differentiate between apoptotic and necrotic cells by means of flow cytometry. Also, other dyes that bind stoichiometrically to double-stranded DNA, such as 4′,6-diamidino-2-phenylindole dihydrochloride (DAPI) and Hoechst 33342, can be used to measure cell viability. Moreover, these molecules can be employed to label the nuclei of permeabilized cells for fluorescence-based assessments. When examined by fluorescence microscopy, nuclei from normal cells glow brightly and homogeneously and can be easily differentiated from apoptotic nuclei, which display chromatin condensation (nuclear pyknosis, at early stages) or a total segmented morphology (karyorhexis, later during the process ***(22)***.

3.4.1. Analysis of $\Delta\psi_m$ Dissipation

1. 25×10^3 HeLa cells are seeded in 24-well plates (0.5 mL of growth medium per well). After 12–24 h, cells are treated with the desired stimuli.
2. At the end of treatments, cells are collected by trypsinization (300 µL of trypsin/EDTA per well), and spun at 300*g* for 5 min (RT) (*see* **Note 70**).
3. Supernatant is discarded and cells are labeled at 37°C either with 150 n*M* TMRM (emitting in red) or with 40 n*M* $DiOC_6(3)$ (emitting in green) in 200 µL of growth medium (*see* **Notes 71** and **72**).
4. Cytofluorometric acquisitions are performed by means of a conventional cytofluorometer equipped with a single laser for excitation (*see* **Notes 73** and **74**).
5. Analysis should be performed on viable, normal-sized cells by gating a single population with normal forward and side scatter parameters (*see* **Note 75**). Each experiment should be supported by an appropriate set of controls (*see* **Note 76**).

3.4.2. Analysis of Phosphatidylserine Externalization

Apoptosis-related PS translocation to the outer leaflet of plasma membrane is detected by staining the cells with fluorescein isothiocyanate (FITC)-conjugated Annexin V (*see* **Note 77**).

1. HeLa cells are cultured, treated, and collected as described above (*see* **Subheading 3.4.1., steps 1** and **2**, and **Note 70**).
2. Supernatant is discarded and cells are washed in 1 mL of binding buffer and centrifuged at 300*g* for 10 min (RT). Supernatant is removed completely and the washing step is repeated.
3. Cells are resuspended in 100 µL of binding buffer and 10 µL of Annexin V-FITC are added.
4. Samples are carefully mixed and incubated at RT under protection from light for 15 min (*see* **Notes 78** and **79**).

5. Cells are washed by adding 1 mL binding buffer and spun at 300 g for 10 min (RT). Supernatant is discarded and cells are resuspended in 500 µL of binding buffer (*see* **Note 80**).
6. Immediately following, cytofluorometric acquisitions are performed as described above (*see* **Subheading 3.4.1., steps 4** and **5**, and **Notes 72–73, 75, 80,** and **81**).

3.4.3. Determination of Mitochondrial ROS Generation and Local ROS Effects

1. 100×10^3 HeLa cells are cultured in 12-well plates (1 mL of growth medium).
2. Twelve to 24 h later, the desired treatments are administered to the cultures.
3. At the end of stimulation, cells are trypsinized (500 µL trypsin/EDTA per well), and spun at 300*g* for 5 min (RT) (*see* **Note 70**).
4. Upon removal of the supernatant, cells are labeled either with 25 µ*M* HE or with 100 n*M* NAO in 500 µL of culture medium.
5. Labeling is performed at 37°C for 10 min.
6. Then, cytofluorometric acquisitions are performed as described above (*see* **Subheading 3.4.1., steps 4** and **5**, and **Notes 72, 73, 75, 82,** and **83**).

3.4.4. Determination of the Mitochondrial Release of IMS Proteins by Immunofluorescence Microscopy

1. 25×10^3 HeLa cells are seeded in 24-well plates as described above (*see* **Subheading 3.1.1., step 1**). After 12–24 h, cells are treated with the desired stimuli.
2. Following treatments, cells are fixed and permeabilized as described before (*see* **Subheading 3.3.1.1., steps 2** and **3** and **Notes 13–16**).
3. For double staining, cells are then incubated with the rabbit anti-AIF and with the mouse anti-cytochrome *c* primary antibodies (both at 1/100 dilution in 500 µl of BSA buffer). Staining can be performed indifferently at RT for 1 h or at 4°C overnight (*see* **Note 84**).
4. Subsequent washing, staining with anti-mouse and anti-rabbit Alexa Fluor®-conjugated secondary antibodies, and mounting are performed as described above (*see* **Subheading 3.3.1.1., steps 5** and **6** and **Note 64**).
5. Examination is then carried out at the fluorescence microscope by using an oil immersion objective (50–65× magnification). Excitation and emission filters should be selected according to the following absorption/emission peaks: 495/519 nm for Alexa Fluor® 488 (green emission); 578/603 nm for Alexa Fluor® 568 (red emission); 352/461 nm for Hoechst 33342 (blue emission).

A distinct, punctuate cytoplasmic pattern of fluorescence indicates the mitochondrial localization of AIF (red fluorescence) and Cyt *c* (green fluorescence). This can be verified by counterstaining mitochondria with antibodies directed against sessile mitochondrial markers, including OM integral (e.g.,

voltage-dependent anion channel) or matrix proteins (e.g., Hsp60). As an alternative, mitochondria can be prestained with MitoTracker® probes, as detailed above (*see* **Subheading 3.3.2.2.**).

On the contrary, a diffuse staining pattern can be observed upon the mitochondrial release of IMS proteins. Following the release from mitochondria, Cyt *c* is found mainly in the cytosol ***(43)***, whereas AIF accumulates in the nucleus ***(63,79)***. The percentage of cells exhibiting a redistribution of AIF and Cyt *c* should be determined in a statistically meaningful population (*see* **Note 19**).

3.4.5. Caspase 3_a Staining

1. HeLa cells are seeded in 24-well plates, treated, permeabilized, and fixed as detailed above (*see* **Subheading 3.1.1., step 1, Subheading 3.3.1.1., steps 2** and **3,** and **Notes 13–16**).
2. For staining, cells are then incubated with the rabbit anti-caspase-3a (1/100 in 500 µL of BSA buffer). Staining can be performed indifferently at RT for 1 h or at 4°C overnight (*see* **Note 84**).
3. Subsequent washing, staining with anti-rabbit Alexa Fluor®-conjugated secondary antibodies, mounting, and examination are performed as previously detailed (*see* **Subheading 3.3.1.1., steps 5** and **6** and **Note 64, Subheading 3.4.4., step 5**).
4. Caspase-3 activation results in a bright, diffuse cytoplasmic red fluorescence, markedly in contrast with the background signal of negative cells. For each sample, the percentage of positivity for caspase-3a should be quantified in a cell population of statistical relevance (*see* **Note 19**).

3.4.6. Detection of Plasma Membrane Integrity

Dead cells incorporate the so-called vital dyes, that are normally excluded by the barrier given by an intact plasma membrane. One of the most widely used vital dyes is propidium iodide (PI).

1. HeLa cells are cultured, treated, and collected as described above (*see* **Subheading 3.4.1., steps 1** and **2** and **Note 70**).
2. Supernatant is discarded and cells are labeled at 37°C with 1 µg/mL PI in 200 µL of growth medium (*see* **Note 71**).
3. Then, cytofluorometric acquisitions are performed as described above (*see* **Subheading 3.4.1., steps 3–5** and **Notes 72, 73, 75, 80,** and **85**).

3.5. A General Strategy for the Resolution of the Central Silemma of Autophagic Cell Death

As outlined in the introduction to this chapter, one of the major problems raised by the observation of autophagic cell death (type 2 cell death) concerns

causality. Does cell death simply occur *with* autophagy, which would constitute a late and desperate attempt of the cell to adapt to stress? Or is cell death mediated *through* autophagy, meaning that self-eating is one of steps that leads to self-killing? In the case of cells presenting massive autophagic vacuolization followed by plasma membrane barrier and disintegration, cell death should be considered as occurring *through* autophagy *sensu stricto* if all the following requirements are met:

1. Cell death (loss of membrane integrity with positive staining for PI or similar vital dyes) should be preceded by all signs of autophagy (double-membraned vesicles, LC3-GFP aggregation, LC3 proteolytic maturation, increase of the acidic subcellular compartment, enhanced turnover of long-lived proteins, co-localization of lysosomal and mitochondrial or ER markers), and these signs should be inhibitable by siRNAs targeting essential proteins of the process (*atg5*, *atg6/Beclin-1*, *atg10*, *atg12*, *hVps34*).
2. Cell death should occur without unequivocal morphological manifestations of apoptosis (e.g., pyknosis, karyorhexis, shrinkage, and formation of the apoptotic bodies). However, cell death may be linked at late stages to mitochondrial permeabilization and caspase activation. These alterations would indicate that apoptotic effector mechanisms have been activated.
3. Most importantly, cell death in all its possible manifestations (autophagic, apoptotic, or necrotic) should be inhibited by genetic manipulations designed to reduce or suppress the expression of *atg* genes or *hVps34*. Thus, the inhibition of autophagy by specific methods (as opposed to the unspecific pharmacological modulators that are currently available) should prevent cell death and maintain the cells healthy and viable.

If it is possible to substantiate by means of these methods that cells can effectively die *through* autophagy, then it will become a challenging endeavor for future investigation to determine the functional importance of autophagic cell death in tissue homeostasis, remodeling, and pathology.

4. Notes

1. Working dilutions of the inducers and inhibitors of autophagy should be prepared from the stock solutions shortly before use. Intermediate dilutions, when necessary, can be made either in sterile PBS or in growth medium.
2. The minimal time necessary to observe a stimulation of the autophagic process varies according to the inducer from 1 h (e.g., upon stimulation with xestospongin C) up to 12 h (e.g., after depletion of serum and amino acids). Thus, to avoid excessive toxicity, it is recommendable NOT to incubate cells for longer than 36–48 h prior to the quantification of autophagic vacuoles.
3. Contrarily to the manufacturer's instructions (recommending 30–50% of confluence), we found that optimal transfection rates are attained when cells

are slightly more confluent (50–70%). However, excessive confluence (at levels coinciding with a reduction of proliferation) should be carefully avoided, since it results in a significant drop of the efficacy of transfection.

4. When the diluted Oligofectamine™ and the siRNA solution are mixed, the solution may appear cloudy. The same applies to Lipofectamine™ and plasmid solutions.
5. The liposome-mediated siRNA transfection protocol is carried out entirely at RT under a common safety cabinet. However, it is recommendable to keep the tubes containing the stock solutions of siRNAs and Oligofectamine™ in an ice bath (and to return them to storage conditions immediately after use), to avoid the degradation of reagents, and to minimize solvent evaporation (both of which may eventually affect the concentration of the stocks). The same applies to the liposome-mediated transfection of plasmids.
6. The absence of serum is especially important for optimal formation of the Oligofectamine™:siRNA complexes. Nevertheless, contrary to common beliefs, we found that complexes (once properly assembled in serum-free conditions) can be added to cells cultured in complete growth medium without relevant reductions of the transfection efficiency. This practice removes the need for serum addition 4 h after transfection. The same applies to the liposome-mediated transfection of plasmids.
7. Given the very high affinity of transfection complexes for the plasma membrane, they should be added to cells dropwise, by trying to cover the whole surface of the growth medium, in order to avoid intrawell variations of the transfection efficiency.
8. Due to multiple variables, including the efficacy of different siRNAs (also targeting the same transcript) as well as the half-life of target proteins, the time required for optimal knock-down may range from a few hours to several days. As a guideline, we recorded satisfactory levels of downregulation of several proteins involved in autophagy (e.g., Beclin-1, LAMP-2, Atg5, Atg10, Atg12, hVps34) 48 h after transfection. However, it is recommendable to check the kinetics of protein downregulation for each siRNA and specific experimental setting. This should be accomplished both at the mRNA level (by RT-PCR, using the appropriate primers) and at the protein level (by immunoblotting with the specific antibodies).
9. As a negative control, cells transfected with scrambled siRNAs or with siRNAs targeting irrelevant sequences (not found in the cellular genome) should be carried along the experimental procedure and subjected to the same treatments administered to cells transfected with siRNA targeting proteins essential for autophagy.
10. At this stage, the seeding concentration heavily depends on the duration and strength of the subsequent treatments. As a guideline, for treatments of 24 h or less (administered 24 h after plating) we use seed 100×10^3cells in 1 mL of growth medium (12-well plates) or 25×10^3 cells in 0.5 mL of growth medium (24-well plates).

11. We recorded the expression of the LC3-GFP fusion protein already 12 h after transfection. Faster expression is not excluded, but should be controlled in the specific experimental setting.
12. As for siRNAs, an adequate control has to be carried along the entire experimental procedure and treated as samples (cells transfected with the plasmid encoding the LC3-GFP chimeric protein). To this aim, untransfected cells may be used. However, a more stringent control is provided by cells transfected with the empty cloning vector.
13. PFA is toxic by inhalation and should be handled under an appropriate fume hood.
14. Stability of the PFA solution is limited. Accordingly, it should be prepared shortly before use. Once dissolved, it is recommendable to keep PFA on ice bath throughout the experiment.
15. Picric acid (chemical name 2,4,6-trinitrophenol) is a close derivative of trinitrotoluene (TNT) and is toxic and explosive if allowed to dry out. Thus, maximal care should be used when handling picric acid.
16. At washing steps, gentle pipetting is recommended to avoid the detachment of cells from the coverslips.
17. Hoechst 33342 is carcinogenic and mutagenic.
18. While wild-type GFP has two excitation peaks, a major one at 395 nm (in the long UV range) and a smaller one at 478 nm (blue), the red-shifted mutant variant encoded by the plasmid pEGFP-C1 (cloning vector from Clontech Laboratories, Palo Alto, CA) is characterized by a single absorption peak at 488 nm and higher expression in mammalian cells.
19. For quantification purposes, the frequency of cells exhibiting cytoplasmic LC3-GFP aggregation should be determined among (at least) 200 cells. Moreover, the number of AV (green dots) per cell should be counted in a representative sample of (at least) 50 cells. The same considerations about the population size apply to other techniques for AV quantification (e.g., MDC or CMFDA staining), as well as to the assessment of translocation of IMS proteins and caspase-3 activation.
20. L-[U-^{14}C]-Valine is a radiochemical. Its handling and storage should conform to the current safety rules.
21. The prechase period is crucial to get rid of short-lived proteins, which are indeed degraded during this step.
22. At this stage, the use of an autophagy inhibitor provides the required negative control.
23. MDC is an autofluorescent molecule characterized by a relatively weak emission, peaking at 525 nm. However, it has been demonstrated that it behaves as a solvent polarity probe ***(80)*** and that its interaction with membrane lipids (as occurring in AV) enhances by severalfold its emission, while shifting its emission to 498 nm.
24. To distinguish the characteristic vesicular distribution of MDC in autophagosomes, each experiment should be performed and scored with the appropriate controls. To this aim, NF medium combined or not with an autophagy inhibitor of choice may provide positive and negative control conditions, respectively.

25. CMFDA is characterized by an absorption and fluorescence emission maxima of 492 and 517 nm, respectively, as determined in aqueous buffer or methanol. Values may exhibit slight variations in cellular environments.
26. To minimize proteolytic degradation, after washing samples should be kept in ice bath until the addition of loading buffer and boiling or storage.
27. Lysis should be performed in the minimal volume of lysis buffer that allows for total resuspension of the pellets (usually 30 μL will suffice). Lysis may be facilitated by thorough pipetting or quick vortexing. Keeping the lysis buffer volume to a minimum reduces the dilution of the protein content of samples, thus resulting in easier gel loading (*see also* **Note 31**).
28. Lysates may be stored at –20°C for prolonged periods (several months) without significant degradation of protein content.
29. Protein quantification is performed by interpolating a calibration curve that is built from a serial dilution of BSA. BSA standards are rarely (if ever) included in the kits for quantification and should be prepared shortly before use from the BSA stock solution.
30. The amount of proteins that should be loaded onto the polyacrylamide gel for separation depends on the size and expected expression levels of protein of interest. For large or highly expressed proteins, 20 μg may suffice to visualize the corresponding band upon immunoblotting. For small or rare proteins larger amounts (up to 60–80 μg) are required.
31. When the quantity of proteins for loading has been determined, samples that will be separated on the same gel are prepared in the minimal volume, which allows one to load the same amount of proteins for each lysate and the addition of 5X loading buffer (to a final concentration of 1X). Keeping the loading volume to a minimum facilitates the loading procedure. In case of diluted samples, 6–7X loading buffer may be employed.
32. Boiling is performed to complement the denaturating activity of lysis and loading buffers (containing SDS, reducing agents, and calcium chelators), with the aim to break the inter- and intramolecular bonds responsible of the higher-level (tertiary and quaternary) protein structures. This step ensures that the subsequent separation is truly based on the size of protein subunits, with little influence of protein–protein interaction and native structural features.
33. The percentage of acrylamide directly determines the sieving properties of the gel, thus influencing its separation range and resolution. As a guideline, proteins with a molecular weight higher than 100 kDa should be resolved on 5–10% total acrylamide gels, whereas smaller proteins can be separated on gels containing 10–15% acrylamide. To facilitate pouring and subsequent handling, concentrations of acrylamide higher than 15% should be avoided.
34. Monomeric acrylamide is a neurotoxin and suspected carcinogen. Avoid skin contact and inhalation. Always wear gloves and protective clothing and handle nonpolymerized acrylamide solutions under a fume hood.
35. In polyacrylamide gels, TEMED acts as crosslinking agent. Also its concentration influences the final properties of the polymerized gel.

36. TEMED is toxic by inhalation. It should be always handled under a fume hood.
37. APS stock solution (10% in dH_2O) is unstable. Storage at 4°C is possible, but never exceed one week. The use of old APS solutions may result in incomplete polymerization of the acrylamide gel.
38. APS generates the free radicals required for the polymerization of acrylamide, thus acting as the catalyst of the reaction. Accordingly, APS should be added as the last component of the gel solution.
39. This protocol reports the amounts of reagents required for a single gel. These quantities may be readily scaled up to pour more gels from the same starting solution. However, no more than four to six gels should be cast from the same solution, to avoid premature polymerization.
40. Hint: Upon pouring, the gel solution remaining in the tube should not be immediately discarded, but left in contact with air. It will help in determining the polymerization state of the gels.
41. Pouring should be performed quickly, while avoiding the formation of bubbles that would interfere with protein migration.
42. It is recommended to leave at least the upper third of the glass height for the stacking gel.
43. Isopropanol may be substituted with pure water.
44. Polymerization time depends on acrylamide concentration, but usually 10–15 min are sufficient. Prolonged polymerization time or incomplete polymerization may result from an old APS stock (*see also* **Note 38**). Polymerization can be verified by examining the remnant solution in the tube in which the gel solution has been prepared (*see also* **Note 40**).
45. The use of a stacking gel improves the resolution of electrophoresis because it causes proteins to accumulate and stack as a very thin zone at the stacking gel/running gel boundary and because it arranges the proteins according to their order of mobility before their entry into the running gel.
46. The comb (which determines the size of wells) should be selected according to the number and final volume of the samples. 5-, 9-, 10-, and 15-well combs are available, allowing to load approximately 60, 50, 40, and 20 µL of samples, respectively.
47. Importantly, the migration buffer should completely cover the wells but not create a communication between the upper and lower chambers that would compromise the correct electrical flow in the cell.
48. Prestained markers covering different ranges of MW are commercially available and allow for visual follow-up of migration.
49. Before entry in the running gel, voltage should be set at 50–70 mV. Thereafter, voltage can be augmented to 140 mV. It should be kept in mind that higher voltages result in reduced migration time but also in lower resolution.
50. Migration fronts, as indicated by the fast migrating bromophenol blue component of the loading buffer, may be safely run off the gel, if desired.
51. During assembly, special care should be taken to avoid the formation of bubbles (which will interfere with the transfer of proteins) between the various layers of

the "sandwich." To remove bubbles, a common 5-mL pipet can be gently rolled on top of each component, before the addition of the next one.

52. Each transfer cassette allows the insertion of two "sandwiches." To avoid the loss of proteins during the transfer, they should both be oriented in the same fashion (*see also* **Note 53**).
53. If the cassette is inserted with the reverse orientation (membrane between the gel and the cathode), negatively charged proteins will be attracted by the anode across the filter paper sheets and the sponge and eventually be lost in the transfer buffer.
54. Due to the intense current, the transfer apparatus temperature tends to increase excessively, if not controlled. As an alternative to the ice block, the entire transfer procedure can be performed in a cold room (4°C).
55. As an alternative, the transfer can be accomplished overnight at a constant current of 45 mA per membrane.
56. To keep the buffer temperature as homogeneous as possible, the transfer should be performed on top of a magnetic stirrer (gentle stirring).
57. Upon careful rinsing in PBS or dH_2O, sponges can be re-used. Filter papers are discarded.
58. At this stage, problems during the transfer (such as bubbles) can be easily identified. Also, membranes can be wrapped in transparent plastic film and photocopied (or digitalized by scanning) to keep track of the correct transfer.
59. At this step, attention should be paid to ensure the even coverage of the membrane with the chemiluminescent substrate.
60. Photographic films are light sensitive and should be handled only in the dark room until the end of the development processing.
61. Exposure time varies greatly according to the intensity of signals from the HRP-catalyzed chemiluminescent reaction. In turn, this depends on several factors, including the amount of protein in the band, the affinity of primary and secondary antibodies, and the time passed from the incubation of the chemiluminescent substrate. For most proteins, exposure times between 1 and 5 min provide good results. When proteins are small or scarcely expressed (or when the antibodies display reduced affinity), longer exposures (up to 10–12 hours) should be attempted. On the contrary, when proteins are large or well represented in the sample (or when the antibodies exhibit high affinity), a few seconds may be sufficient. Some trials may be required to obtain the correct exposition time. Given the time-dependent decay of the luminescent signal, short exposures should be performed before longer ones.
62. If the band of interest cannot be detected upon overnight exposure, the reagent Supersignal West Femto Maximum Sensitivity Substrate may provide enhanced sensitivity.
63. Loading control should be performed with an antibody directed against a highly represented protein, whose amount is stable in most experimental settings. Usually, GAPDH, α-tubulin, or β-actin are detected as loading control.

64. To avoid photobleaching of the fluorescent antibodies, samples should be protected from light from this step onward.
65. As an alternative, 40 or 100X objectives may also be employed.
66. We detected the colocalization of two fluorescent signals by means of a Zeiss LSM 510 confocal microscope.
67. The dual FITC-Texas Red filter combination allows for the visualization of LC3-GFP (absorption/emission peaks at 488/507 nm) and DsRed2-mito (558/583 nm) fusion proteins, as well as of LysoTracker® Red (577/590 nm), MitoTracker® Red CMXRos (579/599 nm), and the Alexa Fluor® 488 (495/517) and 568 (578/603 nm) fluorochromes.
68. To this aim, we routinely use the free, Java®-based, open-source software ImageJ.
69. Staining times may be extended up to 2 h, according to cell type and/or general conditions of the culture.
70. At this stage, the supernatant of treated cells should not be discarded, to avoid the loss of part of the population detached from the plate upon the treatment. Rather, supernatants should be collected in FACS tubes, to which the corresponding cell suspension will be added after trypsinization.
71. To avoid probe-dependent toxicity to the cells, cytofluorometric acquisitions should be performed within 30 min.
72. When large series of samples are to be analyzed (>12 tubes), the interval between labeling and cytofluorometric analysis should be kept constant.
73. To this aim, we routinely use a Becton Dickinson FACScan cytofluorometer, equipped with an argon ion laser emitting at 488 nm. The following channels are employed for the detection of fluorescent emissions: FL1 for $DiOC_6(3)$, FITC and NAO (also in FL2); FL2 for NAO (also in FL1) and TMRM; FL3 for PI and EthBr (as resulting from HE superoxide anion-mediated oxidation) (*see also* **Notes 74, 80,** and **81**).
74. $DiOC_6(3)$ is characterized by absorption/emission peaks at 484/501 nm, TMRM by maxima at 543/573 nm.
75. As a reminder, the forward light scatter gives an indication on cell size whereas the side scatter is related to several factors, including granularity, refractive index, and shape of the cells.
76. Since the incorporation of $DiOC_6(3)$ and TMRM can be influenced by parameters not related to mitochondria (e.g., cell size, plasma membrane permeability, activity of multidrug resistance pumps, etc.) ***(45,66)***, results can only be interpreted when the difference in staining profiles between different experimental conditions (e.g., control vs. apoptosis) are NOT affected by the incubation with a ionophore causing the complete disruption of $\Delta\Psi_m$. Hence, an adequate set of controls can be prepared by splitting in 2 aliquots each sample, and by preincubating one of the two series with 50–100 μM CCCP for 10–15 min before staining (37°C, 5% CO_2).
77. To this aim, we routinely employ the Annexin V-FITC kit from Miltenyi Biotec, according to the manufacturer's instructions.

78. Protection from light prevents photobleaching of FITC fluorochrome.
79. Higher temperatures or longer incubation times lead to nonspecific labeling.
80. If desired, immediately before cytofluorometric acquisition, 5 µL of a 100 µg/mL solution of PI can be added for the simultaneous detection of cells with ruptured plasma membranes. PI is characterized by absorption/emission peaks at 535/617 nm (*see also* **Note 85**).
81. FITC exhibits an absorption maximum at 494 nm and an emission one at 519 nm.
82. EthBr resulting from the ROS-mediated conversion of HE readily binds to DNA, and this complex is characterized by absorption/emission peaks of 300/603 nm (as opposite to reduced HE, emitting at 420 nm).
83. NAO displays absorption/emission peaks at 500/520 nm.
84. At the same time, nuclear counterstaining can be performed by the addition of 2 µM Hoechst 33342, together with primary antibodies.
85. PI staining may be associated with either $DiOC_6(3)$ or Annexin V to distinguish normal cells (PI^-, $DiOC_6(3)^{high}$, or Annexin V^-), dying cells (PI^-, $DiOC_6(3)^{low}$, or Annexin V^+), and dead cells (PI^+) within the same population.

Acknowledgments

This work has been supported by a special grant from Ligue National contre le cancer, as well as by grants from Agence Nationale de Recherche, Agence Nationale pour la Recherche sur le Sida, Fondation pour la Recherche Médicale, Institut National du Cancer, and European Commission (RIGHT, Active p53, Trans-Death, Death-Train, ChemoRes). Xestospongin B was a kind gift of Dr. Jordi Molgó. We are grateful to Dr. Gérard Pierron (Laboratoire "Réplication de l'ADN et Ultrastructure du Noyau"–Villejuif, France) for his contributions to the section on electronic microscopy. The authors would like also to thank Anne-Laure Pauleau, Yael Zermati, and Shahul Mouhamad (INSERM Unit "Apoptosis, Cancer and Immunity"–Villejuif, France) for invaluable help and suggestions.

References

1. Klionsky, D. J., and Emr, S. D. (2000) Autophagy as a regulated pathway of cellular degradation. *Science* **290**, 1717–1721.
2. Mizushima, N., Ohsumi, Y., and Yoshimori, T. (2002) Autophagosome formation in mammalian cells. *Cell Struct. Funct.* **27**, 421–429.
3. Boya, P., Gonzalez-Polo, R. A., Casares, N., et al. (2005) Inhibition of macroautophagy triggers apoptosis. *Mol. Cell Biol.* **25**, 1025–1040.
4. Klionsky, D. J. (2005) The molecular machinery of autophagy: unanswered questions. *J. Cell Sci.* **118**, 7–18.
5. Ohsumi, Y. (2001) Molecular dissection of autophagy: two ubiquitin-like systems. *Nat Rev Mol. Cell Biol.* **2**, 211–216.

6. Kabeya, Y., Mizushima, N., Ueno, T., et al. (2000) LC3, a mammalian homologue of yeast Apg8p, is localized in autophagosome membranes after processing. *EMBO J*. **19**, 5720–5728.
7. Kihara, A., Kabeya, Y., Ohsumi, Y., and Yoshimori, T. (2001) Beclin-phosphatidylinositol 3-kinase complex functions at the trans-Golgi network. *EMBO Rep*. **2**, 330–335.
8. Pattingre, S., Tassa, A., Qu, X., et al. (2005) Bcl-2 antiapoptotic proteins inhibit Beclin 1-dependent autophagy. *Cell* **122**, 927–939.
9. Mizushima, N. (2005) The pleiotropic role of autophagy: from protein metabolism to bactericide. *Cell Death Differ*. **12 (Suppl. 2)**, 1535–1541.
10. Yorimitsu, T., and Klionsky, D. J. (2005) Autophagy: molecular machinery for self-eating. *Cell Death Differ*. **12 (Suppl. 2)**, 1542–1552.
11. Golstein, P., and Kroemer, G. (2007) Cell death by necrosis: towards a molecular definition. *Trends Biochem. Sci*., in press.
12. Gonzalez-Polo, R. A., Boya, P., Pauleau, A. L., et al. (2005) The apoptosis/autophagy paradox: autophagic vacuolization before apoptotic death. *J. Cell. Sci*. **118**, 3091–3102.
13. Yamamoto, A., Tagawa, Y., Yoshimori, T., Moriyama, Y., Masaki, R., and Tashiro, Y. (1998) Bafilomycin A1 prevents maturation of autophagic vacuoles by inhibiting fusion between autophagosomes and lysosomes in rat hepatoma cell line, H-4-II-E cells. *Cell Struct. Funct*. **23**, 33–42.
14. Lum, J. J., Bauer, D. E., Kong, M., et al. (2005) Growth factor regulation of autophagy and cell survival in the absence of apoptosis. *Cell* **120**, 237–248.
15. Boya, P., Gonzalez-Polo, R. A., Poncet, D., et al. (2003) Mitochondrial membrane permeabilization is a critical step of lysosome-initiated apoptosis induced by hydroxychloroquine. *Oncogene* **22**, 3927–3936.
16. Yu, L. Y., Jokitalo, E., Sun, Y. F., et al. (2003) GDNF-deprived sympathetic neurons die via a novel nonmitochondrial pathway. *J. Cell Biol*. **163**, 987–997.
17. Mills, K. R., Reginato, M., Debnath, J., Queenan, B., and Brugge, J. S. (2004) Tumor necrosis factor-related apoptosis-inducing ligand (TRAIL) is required for induction of autophagy during lumen formation in vitro. *Proc. Natl. Acad. Sci. USA* **101**, 3438–3443.
18. Yu, L., Alva, A., Su, H., et al. (2004) Regulation of an ATG7-beclin 1 program of autophagic cell death by caspase-8. *Science* **304**, 1500–1502.
19. Shimizu, S., Kanaseki, T., Mizushima, N., et al. (2004) Role of Bcl-2 family proteins in a non-apoptotic programmed cell death dependent on autophagy genes. *Nat. Cell Biol*. **6**, 1221–1228.
20. Pyo, J. O., Jang, M. H., Kwon, Y. K., et al. (2005) Essential roles of Atg5 and FADD in autophagic cell death: dissection of autophagic cell death into vacuole formation and cell death. *J. Biol. Chem*. **280**, 20722–20729.
21. Marchetti, P., Castedo, M., Susin, S. A., et al. (1996) Mitochondrial permeability transition is a central coordinating event of apoptosis. *J. Exp. Med*. **184**, 1155–1160.
22. Kroemer, G., El-Deiry, W. S., Golstein, P., et al. (2005) Classification of cell death: recommendations of the Nomenclature Committee on Cell Death. *Cell Death Differ*. **12 (Suppl. 2)**, 1463–1467.

23. Debnath, J., Baehrecke, E. H., and Kroemer, G. (2005) Does autophagy contribute to cell death? *Autophagy* **1**, 66–74.
24. Codogno, P., and Meijer, A. J. (2005) Autophagy and signaling: their role in cell survival and cell death. *Cell Death Differ*. **12 (Suppl. 2)**, 1509–1518.
25. Lum, J. J., DeBerardinis, R. J., and Thompson, C. B. (2005) Autophagy in metazoans: cell survival in the land of plenty. *Nat. Rev. Mol. Cell Biol*. **6**, 439–448.
26. Sarbassov, D. D., Ali, S. M., and Sabatini, D. M. (2005) Growing roles for the mTOR pathway. *Curr. Opin. Cell Biol*. **17**, 596–603.
27. Castedo, M., Ferri, K. F., and Kroemer, G. (2002) Mammalian target of rapamycin (mTOR): pro- and anti-apoptotic. *Cell Death Differ*. **9**, 99–100.
28. Asnaghi, L., Bruno, P., Priulla, M., and Nicolin, A. (2004) mTOR: a protein kinase switching between life and death. *Pharmacol. Res*. **50**, 545–549.
29. Petiot, A., Ogier-Denis, E., Blommaart, E. F., Meijer, A. J., and Codogno, P. (2000) Distinct classes of phosphatidylinositol 3′-kinases are involved in signaling pathways that control macroautophagy in HT-29 cells. *J. Biol. Chem*. **275**, 992–998.
30. Zeng, X., Overmeyer, J. H., and Maltese, W. A. (2006) Functional specificity of the mammalian Beclin-Vps34 PI 3-kinase complex in macroautophagy versus endocytosis and lysosomal enzyme trafficking. *J. Cell. Sci*. **119**, 259–270.
31. Scarlatti, F., Bauvy, C., Ventruti, A., et al. (2004) Ceramide-mediated macroautophagy involves inhibition of protein kinase B and upregulation of beclin 1. *J. Biol. Chem*. **279**, 18384–18391.
32. Sarkar, S., Floto, R. A., Berger, Z., et al. (2005) Lithium induces autophagy by inhibiting inositol monophosphatase. *J. Cell Biol*. **170**, 1101–1111.
33. Criollo, A., Maiuri, M. C., Tasdemir, E., et al. (2007) Regulation of autophagy by the inositol trisphosphate receptor. *Cell Death Diff*.**,** in press.
34. Ogata, M., Hino, S. I., Saito, A., et al. (2006) Autophagy is activated for cell survival after ER stress. *Mol. Cell Biol*., in press.
35. Kiffin, R., Bandyopadhyay, U., and Cuervo, A. M. (2006) Oxidative stress and autophagy. *Antioxid. Redox Signal*. **8**, 152–162.
36. Kroemer, G., and Jaattela, M. (2005) Lysosomes and autophagy in cell death control. *Nat. Rev. Cancer* **5**, 886–897.
37. Yoshimori, T., Yamamoto, A., Moriyama, Y., Futai, M., and Tashiro, Y. (1991) Bafilomycin A1, a specific inhibitor of vacuolar-type H(+)-ATPase, inhibits acidification and protein degradation in lysosomes of cultured cells. *J. Biol. Chem*. **266**, 17707–17712.
38. Blommaart, E. F., Krause, U., Schellens, J. P., Vreeling-Sindelarova, H., and Meijer, A. J. (1997) The phosphatidylinositol 3-kinase inhibitors wortmannin and LY294002 inhibit autophagy in isolated rat hepatocytes. *Eur. J. Biochem*. **243**, 240–246.
39. Xue, L., Borutaite, V., and Tolkovsky, A. M. (2002) Inhibition of mitochondrial permeability transition and release of cytochrome c by anti-apoptotic nucleoside analogues. *Biochem. Pharmacol*. **64**, 441–449.
40. Moriyama, Y., and Nelson, N. (1989) H+-translocating ATPase in Golgi apparatus. Characterization as vacuolar H+-ATPase and its subunit structures. *J. Biol. Chem*. **264**, 18445–18450.

41. Bampton, E. T., Goemans, C. G., Niranjan, D., Mizushima, N., and Tolkovsky, A. M. (2005) The dynamics of autophagy visualized in live cells: from autophagosome formation to fusion with endo/lysosomes. *Autophagy* **1**, 23–36.
42. Kroemer, G., Galluzzi, L., and Brenner, C. (2007) Mitochondrial membrane permeabilization in cell death. *Physiol. Rev*. **87**, 99–163.
43. Garrido, C., Galluzzi, L., Brunet, M., Puig, P. E., Didelot, C., and Kroemer, G. (2006) Mechanisms of cytochrome c release from mitochondria. *Cell Death Differ*. **13**, 1423–1433.
44. Chernyak, B. V., Izyumov, D. S., Lyamzaev, K. G., et al. (2006) Production of reactive oxygen species in mitochondria of HeLa cells under oxidative stress. *Biochim. Biophys. Acta* **1757**, 525–534.
45. Zamzami, N., Marchetti, P., Castedo, M., et al. (1995) Sequential reduction of mitochondrial transmembrane potential and generation of reactive oxygen species in early programmed cell death. *J. Exp. Med*. **182**, 367–377.
46. Priault, M., Salin, B., Schaeffer, J., Vallette, F. M., di Rago, J. P., and Martinou, J. C. (2005) Impairing the bioenergetic status and the biogenesis of mitochondria triggers mitophagy in yeast. *Cell Death Differ*. **12**, 1613–1621.
47. Matz, M. V., Fradkov, A. F., Labas, Y. A., et al. (1999) Fluorescent proteins from nonbioluminescent Anthozoa species. *Nat. Biotechnol*. **17**, 969–973.
48. Rizzuto, R., Brini, M., Pizzo, P., Murgia, M., and Pozzan, T. (1995) Chimeric green fluorescent protein as a tool for visualizing subcellular organelles in living cells. *Curr. Biol*. **5**, 635–642.
49. Rizzuto, R., Nakase, H., Darras, B., et al. (1989) A gene specifying subunit VIII of human cytochrome c oxidase is localized to chromosome 11 and is expressed in both muscle and non-muscle tissues. *J. Biol. Chem*. **264**, 10595–10600.
50. Poot, M., Zhang, Y. Z., Kramer, J. A., et al. (1996) Analysis of mitochondrial morphology and function with novel fixable fluorescent stains. *J. Histochem. Cytochem*. **44**, 1363–1372.
51. Daugas, E., Susin, S. A., Zamzami, N., et al. (2000) Mitochondrio-nuclear translocation of AIF in apoptosis and necrosis. *FASEB J*. **14**, 729–739.
52. Galluzzi, L., Zamzami, N., De La Motte Rouge, T., Lemaire, C., Brenner, C., and Kroemer, G. (2007) Methods for the assessment of mitochondrial membrane permeabilization in apoptosis. *Apoptosis*, In press.
53. Obeid, M., Tesniere, A., Ghiringhelli, F., et al. (2007) Calreticulin exposure dictates the immunogenicity of cancer cell death. *Nat. Med*., in press.
54. Kroemer, G., and Reed, J. C. (2000) Mitochondrial control of cell death. *Nat. Med*. **6**, 513–519.
55. Wei, M. C., Zong, W. X., Cheng, E. H., et al. (2001) Proapoptotic BAX and BAK: a requisite gateway to mitochondrial dysfunction and death. *Science* **292**, 727–730.
56. Willis, S. N., and Adams, J. M. (2005) Life in the balance: how BH3-only proteins induce apoptosis. *Curr. Opin. Cell Biol*. **17**, 617–625.
57. Zamzami, N., Larochette, N., and Kroemer, G. (2005) Mitochondrial permeability transition in apoptosis and necrosis. *Cell Death Differ*. **12 (Suppl. 2)**, 1478–1480.

58. Zoratti, M., and Szabo, I. (1995) The mitochondrial permeability transition. *Biochim. Biophys. Acta* **1241**, 139–176.
59. Cain, K., Bratton, S. B., and Cohen, G. M. (2002) The Apaf-1 apoptosome: a large caspase-activating complex. *Biochimie* **84**, 203–214.
60. Martins, L. M., Iaccarino, I., Tenev, T., et al. (2002) The serine protease Omi/HtrA2 regulates apoptosis by binding XIAP through a reaper-like motif. *J. Biol. Chem.* **277**, 439–444.
61. Du, C., Fang, M., Li, Y., Li, L., and Wang, X. (2000) Smac, a mitochondrial protein that promotes cytochrome c-dependent caspase activation by eliminating IAP inhibition. *Cell* **102**, 33–42.
62. Verhagen, A. M., Ekert, P. G., Pakusch, M., et al. (2000) Identification of DIABLO, a mammalian protein that promotes apoptosis by binding to and antagonizing IAP proteins. *Cell* **102**, 43–53.
63. Modjtahedi, N., Giordanetto, F., Madeo, F., and Kroemer, G. (2006) Apoptosis-inducing factor: vital and lethal. *Trends Cell Biol.* **16**, 264–272.
64. Susin, S. A., Lorenzo, H. K., Zamzami, N., et al. (1999) Molecular characterization of mitochondrial apoptosis-inducing factor. *Nature* **397**, 441–446.
65. Li, L. Y., Luo, X., and Wang, X. (2001) Endonuclease G is an apoptotic DNase when released from mitochondria. *Nature* **412**, 95–99.
66. Metivier, D., Dallaporta, B., Zamzami, N., et al. (1998) Cytofluorometric detection of mitochondrial alterations in early CD95/Fas/APO-1-triggered apoptosis of Jurkat T lymphoma cells. Comparison of seven mitochondrion-specific fluorochromes. *Immunol. Lett.* **61**, 157–163.
67. Ferri, K. F., Jacotot, E., Blanco, J., Este, J. A., and Kroemer, G. (2000) Mitochondrial control of cell death induced by HIV-1-encoded proteins. *Ann. NY Acad. Sci.* **926**, 149–164.
68. Susin, S. A., Larochette, N., Geuskens, M., and Kroemer, G. (2000) Purification of mitochondria for apoptosis assays. *Methods. Enzymol.* **322**, 205–208.
69. Goldstein, J., Waterhouse, N., Juin, P., Evan, G., and Green, D. (2000) The coordinate release of cytochrome c during apoptosis is rapid, complete and kinetically invariant. *Nat. Cell Biol.* **2**, 156–162.
70. Loeffler, M., Daugas, E., Susin, S. A., et al. (2001) Dominant cell death induction by extramitochondrially targeted apoptosis-inducing factor. *FASEB J.* **15**, 758–767.
71. Emoto, K., Toyama-Sorimachi, N., Karasuyama, H., Inoue, K., and Umeda, M. (1997) Exposure of phosphatidylethanolamine on the surface of apoptotic cells. *Exp. Cell Res.* **232**, 430–434.
72. Martin, S. J., Reutelingsperger, C. P., McGahon, A. J., et al. (1995) Early redistribution of plasma membrane phosphatidylserine is a general feature of apoptosis regardless of the initiating stimulus: inhibition by overexpression of Bcl-2 and Abl. *J. Exp. Med.* **182**, 1545–1556.
73. Rothe, G., and Valet, G. (1990) Flow cytometric analysis of respiratory burst activity in phagocytes with hydroethidine and 2',7'-dichlorofluorescin. *J. Leukoc. Biol.* **47**, 440–448.

74. Carter, W. O., Narayanan, P. K., and Robinson, J. P. (1994) Intracellular hydrogen peroxide and superoxide anion detection in endothelial cells. *J. Leukoc. Biol*. **55**, 253–258.
75. Petit, P. X., Lecoeur, H., Zorn, E., Dauguet, C., Mignotte, B., and Gougeon, M. L. (1995) Alterations in mitochondrial structure and function are early events of dexamethasone-induced thymocyte apoptosis. *J. Cell Biol*. **130**, 157–167.
76. Kroemer, G., and Martin, S. J. (2005) Caspase-independent cell death. *Nat. Med.* **11**, 725–730.
77. Garrido, C., and Kroemer, G. (2004) Life's smile, death's grin: vital functions of apoptosis-executing proteins. *Curr. Opin. Cell Biol*. **16**, 639–646.
78. Fuentes-Prior, P., and Salvesen, G. S. (2004) The protein structures that shape caspase activity, specificity, activation and inhibition. *Biochem. J*. **384**, 201–232.
79. Vahsen, N., Cande, C., Dupaigne, P., et al. (2006) Physical interaction of apoptosis-inducing factor with DNA and RNA. *Oncogene* **25**, 1763–1774.
80. Niemann, A., Takatsuki, A., and Elsasser, H. P. (2000) The lysosomotropic agent monodansylcadaverine also acts as a solvent polarity probe. *J. Histochem. Cytochem*. **48**, 251–258.
81. Harborth, J., Elbashir, S. M., Bechert, K., Tuschl, T., and Weber, K. (2001) Identification of essential genes in cultured mammalian cells using small interfering RNAs. *J. Cell. Sci*. **114**, 4557–4565.
82. Nobukuni, T., Joaquin, M., Roccio, M., et al. (2005) Amino acids mediate mTOR/raptor signaling through activation of class 3 phosphatidylinositol 3OH-kinase. *Proc. Natl. Acad. Sci. USA* **102**, 14238–14243.